DOI: 10.1021/ic900816h

Inorganic Chemistry
Article

Polymorphism and Inclusion Properties of Three-Dimensional Metal-Organometallic Frameworks Derived from a Terephthalate Sandwich Compound

Sayon A. Kumalah and K. Travis Holman*

Department of Chemistry, Georgetown University, Washington, District of Columbia 20057

Received April 28, 2009

An organometallic sandwich compound of terephthalic acid, namely, $[(\eta^5\text{-Cp})Fe^{II}\{\eta^6\text{-}(1,4\text{-}C_6H_4(COOH)_2)\}]^+$ ($H_2\mathbf{1}^+$), is reported, along with X-ray single crystal structures of $[H\mathbf{1}\cdot H_2\mathbf{1}][PF_6]$ and H**1**. $[H_2\mathbf{1}\cdot H\mathbf{1}][PF_6]$ was reacted with the nitrate salts of Co^{II} and Ni^{II} to yield a series of three-dimensional (3D) metal-organometallic framework (MOMF) materials of the composition $[M_3(\mathbf{1})_4(\mu\text{-}H_2O)_2(H_2O)_2][NO_3]_2\cdot x$solvent (M = Co^{II} (**2**), Ni^{II} (**3**); *x*solvent = 4EtOH, or $2DMF\cdot 2H_2O$). These framework structures were shown by single crystal and powder X-ray diffraction to be polymorphic, possessing identical 3D body-centered tetragonal network topologies, but differing in the manner by which the $[CpFe]^+$ groups are arranged within the two-dimensional, square grid sheets of the 3D networks. **α-2-EtOH**, ***β*-2-EtOH**, **α-3-EtOH**, ***β*-2-DMF**, and ***β*-3-DMF** were thermally desolvated, giving rise to isolable apohosts of composition $[M_3(\mathbf{1})_4(\mu\text{-}H_2O)_2(H_2O)_2][NO_3]_2$ (M = Co^{II} (**2**), Ni^{II} (**3**)) that were shown by PXRD to possess different, as yet unknown, crystal structures. The desolvated apohosts were studied with respect to their ability to selectively reabsorb water and/or alcohols. They show a modest preference for the absorption of water and short chain, linear alcohols (<C4), with modest selectivity for 1-PrOH.

Introduction

The synthesis and study of coordination polymers and metal-organic frameworks (MOFs) has grown into a highly active area of research over the past several years.[1] Materials of this burgeoning class exhibit industrially relevant properties such as crystallinity and permanent porosity,[1f,1g,2] and are highly amenable to design,[3] characteristics that bode well for their potential use in applications such as gas storage,[4] catalysis,[5] separations,[6] and sensing,[7] among others. In terms of design, there is growing emphasis on the synthesis of framework materials possessing multifunctional ligands, that is, ligands that can be used to sustain the framework architecture while concomitantly introducing moieties that convey

*To whom correspondence should be addressed. E-mail: kth7@georgetown.edu.

(1) (a) Robson, R. *Dalton Trans*. **2008**, *38*, 5113. (b) Rowsell, J.; Yaghi, O. *Microporous Mesoporous Mater*. **2004**, *73*, 3. (c) Rosseinsky, M. *Microporous Mesoporous Mater*. **2004**, *73*, 15. (d) Kitagawa, S.; Kitaura, R.; Noro, S. *Angew. Chem., Int. Ed.* **2004**, *43*, 2334. (e) James, S. *Chem. Soc. Rev*. **2003**, *32*, 276. (f) Papaefstathiou, G.; MacGillivray, L. *Coord. Chem. Rev*. **2003**, *246*, 169. (g) Yaghi, O.; O'Keeffe, M.; Ockwig, N.; Chae, H.; Eddaoudi, M.; Kim, J. *Nature* **2003**, *423*, 705. (h) Maji, T.; Kitagawa, S. *Pure Appl. Chem*. **2007**, *79*, 2155. (i) Moulton, B.; Zaworotko, M. *Chem. Rev*. **2001**, *101*, 1629. (j) Batten, K.; Robson, R. *Angew. Chem., Int. Ed*. **1998**, *37*, 1460. (k) Ferey, G. *Chem. Soc. Rev*. **2008**, *37*, 191.

(2) (a) Eddaoudi, M.; Moler, D.; Li, H.; Chen, B.; Reineke, T. M.; O'Keeffe, M.; Yaghi, O. *Acc. Chem. Res*. **2001**, *34*, 319. (b) Janiak, C. *Dalton Trans*. **2003**, *14*, 2781.

(3) (a) Bureekaew, S.; Shimomura, S.; Kitagawa, S. *Sci. Technol. Adv. Mater*. **2008**, *9*.(b) Halder, G. J.; Kepert, C. *Aus. J. Chem*. **2006**, *59*, 597. (c) Suh, M.; Cheon, Y.; Lee, E. *Coord. Chem. Rev*. **2008**, *252*, 1007. (d) Kawano, M.; Fujita, M. *Coord. Chem. Rev*. **2007**, *251*, 2592.

(4) (a) Roswell, J. L.; Yaghi, O. *Angew. Chem., Int. Ed.* **2005**, *44*, 4670. (b) Collins, D.; Zhou, H.-C. *J. Mater. Chem*. **2007**, *17*, 3154. (c) Kitagawa, S.; Matsuda, R. *Coord. Chem. Rev*. **2007**, *251*, 2490. (d) Dybtsev, D.; Chun, H.; Yoon, S.-H.; Kim, D.; Kim, K. *J. Am. Chem. Soc*. **2004**, *126*, 5666. (e) Dinca, M.; Long, J. *Angew. Chem., Int. Ed*. **2008**, *47*, 6766. (f) Belof, J.; Stern, A.; Eddaoudi, M.; Space, B. *J. Am. Chem. Soc*. **2007**, *129*, 15202–15210.

(5) (a) Fujita, M.; Kwon, Y.-J.; Washizu, S.; Ogura, K. *J. Am. Chem. Soc*. **1994**, *116*, 1151. (b) Seo, J.; Whang, D.; Lee, H.; Jun, S.; Oh, J.; Jeon, Y.; Kim, K. *Nature* **2000**, *404*, 982. (c) Wu, C. −D.; Hu, A.; Zhang, L.; Lin, W. *J. Am. Chem. Soc*. **2005**, *127*, 8940. (d) Wu, C.-D.; Lin, W. *Angew. Chem., Int. Ed*. **2007**, *46*, 1075. (e) Dybtsev, D.; Nuzhdin, A.; Chun, H.; Bryliakov, K.; Talsi, E. P.; Fedin, V. P.; Kim, K. *Angew. Chem., Int. Ed*. **2006**, *45*, 916. (f) Cho, S.-H.; Gadzikwa, T.; Afshari, M.; Nguyen, S.; Hupp, J. *Eur. J. Inorg. Chem*. **2007**, *31*, 4863. (g) Cho, S.-H.; Ma, B.; Nguyen, S. T.; Hupp, J. T.; Albrecht-Schmitt, T. E. *Chem. Commun*. **2006**, *24*, 2563. (h) Alkordi, M.; Liu, Y.; Larsen, R.; Eubank, J.; Eddaoudi, M. *J. Am. Chem. Soc*. **2008**, *130*, 12639.

(6) (a) Pan, L.; Olson, D.; Ciemnolonski, L. R.; Heddy, R.; Li, J. *Angew. Chem., Int. Ed*. **2005**, *44*, 1. (b) Chen, B.; Liang, C.; Yang, J.; Contreras, D.; Clancy, Y.; Lobkovsky, E.; Yaghi, O.; Dai, S. *Angew. Chem., Int. Ed*. **2006**, *45*, 1390. (c) Dybtsev, D.; Chun, H.; Yoon, S.; Kim, D.; Kim, K. *J. Am. Chem. Soc*. **2004**, *126*, 32. (d) Custelcean, R.; Gorbunova, M. *J. Am. Chem. Soc*. **2005**, *39*, 13519. (e) Bourrelly, S.; Llewellyn, P.; Serre, C.; Millange, F.; Loiseau, T.; Ferey, G. *J. Am. Chem. Soc*. **2005**, *39*, 13519.

(7) (a) Chen, B.; Yang, Y.; Zapata, F.; Lin, G.; Qian, G.; Lobkovsky, E. *Adv. Mater*. **2007**, *19*, 1693. (b) Wong, K.-L.; Law, G.-L.; Yang, Y.-Y.; Wong, W.-T. *Adv. Mater*. **2006**, *18*, 1051. (c) Maspoch, D.; Ruiz-Molina, D.; Wurst, K.; Domingo, N.; Cavallini, M.; Biscarini, F.; Tejada, J.; Rovira, C.; Veciana, J. *Nat. Mater*. **2003**, *2*, 190. (d) Halder, G.; Kepert, C.; Moubaraki, B.; Murray, K.; Cashion, J. *Science* **2002**, *298*, 1762.

Published on Web 05/27/2009

functional properties to the material (e.g., recognition,[8] chiroselectivity,[5b−5g,9] catalytic,[5] sensory,[10] Lewis acidic[11] or basic sites,[5b,12] and so forth). Strategically functionalized frameworks can be achieved by direct synthesis from appropriately functionalized ligands, or, if synthetic limitations exist, via postsynthetic covalent modification of the ligands,[13] whereby functional groups that line the inner surface of the material are chemically modified to engender properties of interest.

Considering recent efforts in organometallic crystal engineering[14] and the importance of organometallics in chemistry at large, the use of organometallic bridging ligands (i.e., ligands possessing a metal−carbon bond) in the propagation of two-dimensional (2D) and three-dimensional (3D) framework materials has obvious potential, yet remains an area that is relatively underdeveloped. Indeed, organometallic bridging ligands, building blocks for what could appropriately be termed "metal-organometallic frameworks (MOMFs)", may be chosen so as to exploit diverse chemical features ranging from charge, red-ox activity, photochemical activity, magnetic behavior, or catalytic activity. Examples of known MOMFs derived from organometallic bridging ligands illustrate nicely their potential as functional materials.[15] Metallocyanide ligands, for example, have long been used to construct heterometallic MOMFs,[16] many of which exhibit sustainable porosity[17] and/or notable magnetic properties.[18] Metallocene-based bridging ligands have also been commonly exploited, giving rise to, for example, redox active MOMFs.[19] Sweigart and co-workers have synthesized a series of MOMFs from π-bonded transition metal quinoid complexes, some members of which are known homogeneous catalysts.[20] Still others have exploited metalloligands, of which organometallic ligands are a subset, in the design of heterometallic frameworks,[21] some of which form transient organometallic species during their function as heterogeneous catalysts.[5b−5g]

Arene carboxylate ligands, especially terephthalate (1,4-benzene-dicarboxylate, hereafter 1,4-bdc),[22−24] are the literal

(8) (a) Chen, B.; Wang, L.; Zapata, F.; Qian, G.; Lobkovsky, E. B. *J. Am. Chem. Soc.* **2008**, *130*, 6718. (b) Custelcean, R.; Moyer, B. *Eur. J. Inorg. Chem.* **2007**, *10*, 1321. (c) Custelcean, R.; Gorbunova, M. *J. Am. Chem. Soc.* **2005**, *127*, 16362. (d) Zhao, B.; Gao, H.-L.; Chen, X.-Y.; Cheng, P.; Shi, W.; Liao, D.-Z.; Yan, S.-P.; Jiang, Z.-H. *Chem.—Eur. J.* **2006**, *12*, 149. (e) Custelcean, R.; Remy, P.; Bonnesen, P.; Jiang, D.-e.; Moyer, B. *Angew. Chem., Int. Ed.* **2004**, *47*, 1886. (f) Zhao, B.; Chen, X.-Y.; Cheng, P.; Liao, D.-Z.; Yan, S.-P.; Jiang, Z.-H. *J. Am. Chem. Soc.* **2004**, *126*, 15934. (g) Liu, W.; Jiao, T.; Li, Y.; Liu, Q.; Tan, M.; Wang, H.; Wang, L. *J. Am. Chem. Soc.* **2004**, *126*, 2280. (h) Mough, S.; Holman, K. *Chem. Commun.* **2008**, *12*, 1407–109. (i) Ugono, O.; Moran, J.; Holman, K. *Chem. Commun.* **2008**, *12*, 1404–1406.

(9) (a) Lin, W. *MRS Bull.* **2007**, *32*, 544–548. (b) Dybtsev, D.; Nuzhdin, A.; Chun, H.; Bryliakov, K.; Talsi, E.; Fedin, V.; Kim, K. *Angew. Chem., Int. Ed.* **2006**, *45*, 916. (c) Kesanli, B.; Lin, W. *Coord. Chem. Rev.* **2003**, *246*, 305. (d) Lin, W. *J. Solid State Chem.* **2005**, *178*, 2486. (e) Pecoraro, V.; Bodwin, J.; Cutland, A. *J. Solid State Chem.* **2000**, *152*, 68. (f) Bradshaw, D.; Claridge, J.; Cussen, E.; Prior, T.; Rosseinsky, M. *Acc. Chem. Res.* **2005**, *38*, 273. (g) Evans, O.; Ngo, H.; Lin, W. *J. Am. Chem. Soc.* **2001**, *123*, 10395. (h) Xiong, R.-G.; You, X.-Z; Abrahams, B.; Xue, Z.; Che, C.-M. *Angew. Chem., Int. Ed.* **2001**, *40*, 4422.

(10) (a) Montes, V.; Zyryanov, G.; Danilov, E.; Agarwal, N.; Palacios, M.; Anzenbacher, P. *J. Am. Chem. Soc.* **2009**, *131*, 1787–1795. (b) Qiu, L.-G.; Li, Z.-Q.; Wu, Y.; Wang, W.; Xu, T.; Jiang, X. *Chem. Commun.* **2008**, *31*, 3642–3644. (c) Harbuzaru, B.; Corma, A.; Rey, F.; Atienzar, P.; Jorda, J.; Garcia, H.; Ananias, D.; Carlos, L.; Rocha, J. *Angew. Chem., Int. Ed.* **2008**, *47*, 1080–1083. (d) Shimomura, S.; Matsuda, R.; Tsujino, T.; Kawamura, T.; Kitagawa, S. *J. Am. Chem. Soc.* **2006**, *128*, 16416–16417. (e) Chandler, B.; Cramb, D.; Shimizu, G. *J. Am. Chem. Soc.* **2006**, *128*, 10403.

(11) (a) Horike, S.; Dinca, M.; Tamaki, K.; Long, J. *J. Am. Chem. Soc.* **2008**, *130*, 5854–5855. (b) Alaerts, L.; Seguin, E.; Poelman, H.; Thibault-Starzyk, F.; Jacobs, P. A.; De Vos, D. *Chem.—Eur. J.* **2006**, *12*, 7353–7363. (c) Guo, X.; Zhu, G.; Li, Z.; Sun, F.; Yang, Z.; Qiu, S. *Chem. Commun.* **2006**, *30*, 3172–3174. (d) Schlichte, K.; Kratzke, T.; Kaskel, S. *Microporous Mesoporous Mater.* **2004**, *73*, 81–88. (e) Noro, S.-i.; Horike, S.; Tanaka, D.; Kitagawa, S.; Akutagawa, T.; Nakamura, T. *Inorg. Chem.* **2006**, *45*, 9290–9300.

(12) (a) Chen, B.; Wang, L.; Xiao, Y.; Fronczek, F.; Xue, M.; Cui, Y.; Qian, G. *Angew. Chem., Int. Ed.* **2009**, *48*, 500–503. (b) Horike, S.; Bureekaew, S.; Kitagawa, S. *Chem. Commun.* **2008**, *4*, 471–473. (c) Higuchi, M.; Horike, S.; Kitagawa, S. *Supramol. Chem.* **2007**, *19*, 75–78.

(13) (a) Burrows, A.; Frost, C.; Mahon, M.; Richardson, C. *Angew. Chem., Int. Ed.* **2008**, *47*, 8482–8486. (b) Gadzikwa, T.; Lu, G.; Stern, C.; Wilson, S.; Hupp, J.; Nguyen, S. *Chem. Commun.* **2008**, *43*, 5493–5495. (c) Dugan, E.; Wang, Z.; Okamura, M.; Medina, A.; Cohen, S. *Chem. Commun.* **2008**, *29*, 3366–3368. (d) Song, Y.-F.; Cronin, L. *Angew. Chem., Int. Ed.* **2008**, *47*, 4635–4637. (e) Ingleson, M.; Barrio, J.; Guilbaud, J.-B.; Khimyak, Y.; Rosseinsky, M. *Chem. Commun.* **2008**, *23*, 2680–2682. (f) Costa, J.; Gamez, P.; Black, C.; Roubeau, O.; Teat, S.; Reedijk, J. *Eur. J. Inorg. Chem.* **2008**, *10*, 1551–1554. (g) Wang, Z.; Cohen, S. *J. Am. Chem. Soc.* **2007**, *129*, 12368–12369.

(14) (a) Braga, D.; Giaffreda, S.; Grepioni, F.; Pettersen, A.; Maini, L.; Curzi, M.; Polito, M. *Dalton Trans.* **2006**, 1249–1263. (b) Braga, D.; Giaffreda, S.; Grepioni, F.; Maini, L.; Polito, M. *Coord. Chem. Rev.* **2006**, *250*, 1267–1285. (c) Braga, D.; Grepioni, F. *Coord. Chem. Rev.* **1999**, *183*, 19–41. (d) Braga, D.; Grepioni, F.; Desiraju, G. *Chem. Rev.* **1998**, *98*, 1375–1405.

(15) (a) Prokopuk, N.; Shriver, D. *Inorg. Chem.* **1997**, *36*, 5609. (b) Kim, Y.; Verkade, J. *Inorg. Chem.* **2003**, *42*, 4262. (c) Costa, R.; Lopez, C.; Molins, E.; Espinosa, E. *Inorg. Chem.* **1998**, *37*, 5686. (d) Bailey, A.; Shang, M.; Fehlner, T. *Inorg. Chem.* **2000**, *39*, 4374. (e) Hou, H.; Li, G.; Li, L.; Zhu, Y.; Meng, X.; Fan, Y. *Inorg. Chem.* **2003**, *42*, 428. (f) Guo, D.; Mo, H.; Duan, C.; Lu, F.; Meng, Q. *J. Chem. Soc., Dalton Trans.* **2002**, 2593. (g) Yang, Y.-Y.; Wong, W.-T. *Chem. Commun.* **2002**, *22*, 2716.

(16) (a) Hoskins, B.; Robson, R. *J. Am. Chem. Soc.* **1990**, *112*, 1546. (b) Boyer, J.; Kuhlman, M.; Rauchfuss, T. *Acc. Chem. Res.* **2007**, *40*, 233–242. (c) Tanase, S.; Reedijk, J. *Coord. Chem. Rev.* **2006**, *250*, 2501–2510. (d) Ibrahim, A. *J. Mater. Chem.* **1998**, *8*, 841–846.

(17) Chapman, K.; Southon, P.; Weeks, C.; Kepert, C. *Chem. Commun.* **2005**, 3322.

(18) (a) Vos, T.; Liao, Y.; Shum, W.; Her, J.-H.; Stephens, P. W.; Reiff, W.; Miller, J. *J. Am. Chem. Soc.* **2004**, *126*, 11630. (b) Shum, W.; Schaller, J.; Miller, J. *J. Phys. Chem. C.* **2008**, *112*, 7936.

(19) Hayakawa, Y.; Miyazawa, M.; Oyama, A.; Unoura, K.; Kawaguchi, H.; Naito, T.; Maeda, K.; Uchida, F.; Kondo, M. *Inorg. Chem.* **2004**, *43*, 5801.

(20) (a) Oh, M.; Reingold, J.; Carpenter, G.; Sweigart, D. *Coord. Chem. Rev.* **2004**, *248*, 561. (b) Oh, M.; Reingold, J.; Carpenter, G.; Sweigart, D. *J. Organomet. Chem.* **2003**, *687*, 78. (c) Oh, M.; Carpenter, G.; Sweigart, D. *Organometallics* **2002**, *21*, 1290. (d) Oh, M.; Carpenter, G.; Sweigart, D. *Angew. Chem., Int. Ed.* **2001**, *40*, 3191. (e) Oh, M.; Carpenter, G.; Sweigart, D. *Acc. Chem. Res.* **2004**, *37*, 1. (f) Oh, M.; Carpenter, G.; Sweigart, D. *Organometallics* **2003**, *22*, 2364.

(21) (a) Halper, S.; Do, L.; Stork, J.; Cohen, S. *J. Am. Chem. Soc.* **2006**, *128*, 15255. (b) Halper, S.; Cohen, S. *Inorg. Chem.* **2005**, *44*, 486–488. (c) Murphy, D.; Malachowski, M.; Campana, C.; Cohen, S. *Chem. Commun.* **2005**, 5506–5508. (d) Decurtins, S.; Schmalle, H. W.; Schneuwly, P.; Ensling, J.; Gutlich, P. *J. Am. Chem. Soc.* **1994**, *116*, 9521–9528. (e) Sharma, C.; Broker, G.; Huddleston, J.; Baldwin, J.; Metzger, R.; Rogers, R. *J. Am. Chem. Soc.* **1999**, *121*, 1137–1144. (f) Suslick, K.; Bhyrappa, P.; Chou, J.; Kosal, M.; Nakagaki, S.; Smithenry, D.; Wilson, S. *Acc. Chem. Res.* **2005**, *38*, 283. (g) Goldberg, I. *Chem.—Eur. J.* **2000**, *6*, 3863.

(22) A CSD (v. 5.30, Feb. 2009) search for metal-organic polymers sustained by bridging terephthlate (unsubstituted) ligands yielded 164 hits, some of the more impactful of which are cited in refs 23 and 24.

(23) (a) Li, H.; Eddaoudi, M.; O'Keeffe, M.; Yaghi, M. *Nature* **1999**, *402*, 276. (b) Reineke, T.; Eddaoudi, M.; Fehr, M.; Kelley, D.; Yaghi, O. *J. Am. Chem. Soc.* **1999**, *121*, 1651–1657. (c) Rosi, N.; Eckert, J.; Eddaoudi, M.; Vodak, D.; Kim, J.; O'Keeffe, M.; Yaghi, O. *Science* **2003**, *300*, 1127–1129. (d) Eddaoudi, M.; Li, H.; Yaghi, O. *J. Am. Chem. Soc.* **2000**, *122*, 1391–1397. (e) Li, H.; Eddaoudi, M.; Groy, T.; Yaghi, O. *J. Am. Chem. Soc.* **1998**, *120*, 8571–8572.

(24) (a) Ferey, G.; Mellot-Draznieks, C.; Serre, C.; Millange, F.; Dutour, J.; Surble, S.; Margiolaki, I. *Science* **2005**, *309*, 2040–2042. (b) Serre, C.; Millange, F.; Thouvenot, C.; Nogues, M.; Marsolier, G.; Louer, D.; Ferey, G. *J. Am. Chem. Soc.* **2002**, *124*, 13519–13526. (c) Serre, C.; Mellot-Draznieks, C.; Surble, S.; Audebrand, N.; Filinchuk, Y.; Ferey, G. *Science* **2007**, *315*, 1828–1831. (d) Loiseau, T.; Serre, C.; Huguenard, C.; Fink, G.; Taulelle, F.; Henry, M.; Bataille, T.; Ferey, G. *Chem.—Eur. J.* **2004**, *10*, 1373–1382.

Scheme 1

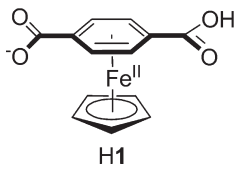

H1

and figurative pillars of MOF chemistry.[1−4] Described herein are the syntheses, structures, polymorphism, and inclusion properties of a series of Co^{II} and Ni^{II} based 3D MOMFs derived from an organometallic sandwich compound of the much-studied terephthalate ligand, namely, the $[(\eta^5\text{-Cp})Fe^{II}]^+$-functionalized ligand $\mathbf{1}^-$ (Scheme 1). Several factors motivated our exploration of $[(\eta^5\text{-Cp})Fe^{II}(\eta^6\text{-arene})]^+$-type[25] sandwich compounds of benzoate ligands, such as $\mathbf{1}^-$, in the design of functionalized MOMFs: (i) such ligands are easily synthesized and available in multigram quantities; (ii) they are highly air, water, and thermally stable compounds and therefore tolerate a range of synthetic conditions; (iii) $[CpFe^{II}(\eta^6\text{-arene})]^+$ compounds are excellent models for $[Cp^xRu^{II}(\eta^6\text{-arene})]^+$ compounds,[26] both of which are photochemically active, liberating $[Cp^xM]^+$ (M = Fe, Ru) moieties as potentially useful (e.g., catalytically active,[27] gas-binding[28]) $[Cp^xM(solvent)_3]^+$ species in the presence of appropriate solvents;[29] (iv) it was of interest to examine the structural influence, if any, that would be exerted by the bulky and positively charged $[CpFe]^+$ moieties. It was conceivable, for instance, that the presence of the $[CpFe]^+$ moiety might lead to some non-"default"[30] framework structures of the terephthalate anion. Moreover, the symmetry of $\mathbf{1}^-$ (C_{2v}) is reduced relative to terephthalate (D_{2h}), giving rise to the possibility of supramolecular[31] (or architectural[32]) framework isomers and/or polymorphs depending on the relative positioning of the $[CpFe]^+$ groups within the resulting MOMFs; v) finally, the coordination chemistry of η^6-coordinated arene carboxylate ligands is as yet unexplored, though during the course of this work Long and coworkers communicated the post-synthetic functionalization of MOF-5[23a] by $Cr(CO)_3$ moieties.[33] The resulting MOMF, namely $Zn_4O[(\eta^6\text{-1,4-benzenedicarboxylate})Cr(CO)_3]_3$, was photochemically activated to release CO and reversibly bind H_2 or N_2 at the coordinatively unsaturated chromium centers, nicely illustrating the potential for MOMF materials derived from metal-functionalized organometallic ligands.

Experimental Section

Materials and Methods. All solvents were used as received from Fisher (Pittsburgh, PA). Reagents were obtained from Acros (Pittsburgh, PA) or Aldrich (Milwaukee, WI) and were used without further purification. $[CpFe(p\text{-xylene})][PF_6]$ was synthesized according to literature procedures.[25a] All reactions were performed in the dark, and manipulations were performed in the presence of minimal ambient light. Elemental analyses were carried out on a Perkin-Elmer PE2400 microanalyzer at Georgetown University. NMR spectra were recorded on either a Mercury Varian 300 MHz or an Inova 400 MHz Spectrometer operating at 300 or 400 MHz (^{1}H), or 75.5 or 100.5 MHz (^{13}C), respectively. ^{1}H and ^{13}C spectra were indirectly referenced to TMS using residual solvent signals as internal standards. Thermogravimetric analyses (TGA) were performed under a constant flow of nitrogen using either a TA Instruments TGA 2050 or Q5000 instrument.

X-ray Crystallography. Single crystal diffraction data were collected using a Siemens SMART 1k CCD X-ray diffractometer with Mo Kα radiation (0.71073 Å) at 173(2) K. The crystal structures were solved by direct methods using SHELXS, and all structural refinements were conducted using SHELXL-97−2.[34] All non-hydrogen atoms were modeled with anisotropic displacement parameters, with the exception of some included solvents and/or disordered moieties (nitrate anions or cyclopentadienyl ligands). Early refinement models of compound **α-2**-EtOH, ***β*-2**-EtOH, and ***β*-3**-DMF indicated the presence of highly disordered included solvents. In these refinements, the SQUEEZE subroutine in PLATON[35] was used to model the electron density associated with the highly disordered species and to confirm the stoichiometry of the included solvent. Summary crystallographic data are given in Table 1. The program X-Seed was used as a graphical interface for the SHELX software suite and for the generation of figures.[36] Powder X-ray diffraction (PXRD) data were collected using a Rigaku R-Axis Rapid diffractometer using graphite monochromated Cu Kα radiation (λ = 1.5418 Å) and a 0.5 mm collimator. Samples were mounted in a 0.5 mm capillary tube and were irradiated typically for 60 min. The diffraction data were analyzed using AreaMax v. 1.15 (5−60° 2θ, with a 0.02° step size) and were further manipulated using MDI Jade 5.0. Background corrections were performed by subtracting the pattern derived from an empty capillary. Temperature regulation of the PXRD samples was achieved using a constant stream of temperature-regulated N_2 gas. CCDC 687392−687398 contain the supplementary crystallographic data for the structures reported herein. These data can be obtained free of charge via http://www.ccdc.cam.ac.uk/conts/retrieving.html, or from the Cambridge Crystallographic Data Centre, 12 Union Road, Cambridge CB2 1EZ, U.K.; fax: (+44) 1223−336−033; or e-mail: deposit@ccdc.cam.ac.uk.

Syntheses. $[H_2\mathbf{1}\cdot\mathbf{H1}][PF_6]$. A 3.0 g portion of $[CpFe(p\text{-xylene})][PF_6]$ (13 mmol) was added to an aqueous solution (300 mL) of 7.9 g (50 mmol) of potassium permanganate. The solution was stirred and refluxed overnight in the dark. The resulting solution was then filtered and concentrated under reduced pressure to about 5.0 mL. Concentrated HCl(aq.) was added dropwise until precipitation ceased. The yellow precipitate was filtered and dried to give 1.2 g, 35% of $[H_2\mathbf{1}\cdot\mathbf{H1}][PF_6]$. Single crystals of $[H_2\mathbf{1}\cdot\mathbf{H1}][PF_6]$ were grown by recrystallization

(25) (a) Nesmeyanov, A.; Vol'kenau, N.; Bolesova, I. *Dokl. Akad. Nauk SSSR* **1963**, *149*, 615. (b) Nesmeyanov, A.; Vol'kenau, N.; Bolesova, I. *Tetrahedron Lett*. **1963**, *25*, 1725. (c) Astruc, D. *Top. Curr. Chem*. **1992**, *160*, 47–95.

(26) (a) Pigge, F.; Coniglio, J. *J. Curr. Org. Chem*. **2001**, *5*, 757–784. (b) Fairchild, R.; Holman, K. *Organometallics* **2008**, *27*, 1823–1833. (c) Fairchild, R. M.; Holman, K. T. *Organometallics* **2007**, *26*, 3049-3053; *Organometallics* **2007**, *26*, 4086.(d) Fairchild, R.; Holman, K. *J. Am. Chem. Soc*. **2005**, *127*, 16364–16365.

(27) Trost, B.; Frederiksen, M.; Rudd, M. *Angew. Chem., Int. Ed*. **2005**, *44*, 6630–6666.

(28) See, for example: Gemel, C.; Huffman, J. C.; Caulton, K. G.; Mauthner, K.; Kirchner, K. *J. Organomet. Chem*. **2000**, *593−594*, 342−353.

(29) (a) Gill, T.; Mann, K. *Organometallics* **1982**, *1*, 485. (b) Gill, T.; Mann, K. *Inorg. Chem*. **1983**, *22*, 1986. (c) Schrenk, J.; McNair, A.; McCormick, F.; Mann, K. *Inorg. Chem*. **1986**, *25*, 3501–3504.

(30) Eddaoudi, M.; Kim, J.; Vodak, D.; Sudik, A.; Wachter, J.; O'Keeffe, M.; Yaghi, O. *Proc. Nat. Acad. Sci*. **2002**, *99*, 4900.

(31) (a) Moulton, B.; Zaworotko, M. *Chem. Rev*. **2001**, *101*, 1629. (b) Abourahma, H.; Moulton, B.; Kravtsov, V.; Zaworotko, M. *J. Am. Chem. Soc*. **2002**, *124*, 9990. (c) Rather, B.; Moulton, B.; Bailey, R.; Zaworotko, M. *Chem. Commun*. **2002**, 7, 694. (d) Moulton, B.; Abourahma, H.; Bradner, M. W.; Lu, J.; McManus, G.; Zaworotko, M. *Chem.Commun*. **2003**, *12*, 1342.

(32) (a) Swift, J.; Pivovar, A.; Reynolds, A.; Ward, M. *J. Am. Chem. Soc*. **1998**, *120*, 5887–5894. (b) Holman, K.; Martin, S.; Parker, P.; Ward, M. *J. Am. Chem. Soc*. **2001**, *123*, 4421–4431. (c) Holman, K.; Swift, J.; Pivovar, A.; Ward, M. *Acc. Chem. Res*. **2001**, *34*, 107–118. (d) Horner, M.; Holman, K.; Ward, M. *J. Am. Chem. Soc*. **2007**, *129*, 14640–14660.

(33) Kaye, S.; Long, J. *J. Am. Chem. Soc*. **2008**, *130*, 806.

(34) Sheldrick, G. *Acta Crystallogr., Sect. A* **1990**, *46*, 467.

(35) Spek, A. *J. Appl. Crystallogr*. **2003**, *36*, 7.

(36) Barbour, L. *Supramol. Chem*. **2001**, *1*, 189; http://x-seed.net.

Table 1. Summary Data from X-ray Single Crystal Structure Determinations

	$[H_2\mathbf{1}\cdot H\mathbf{1}][PF_6]$	**H1**	**α-2-EtOH**	***β*-2-EtOH**	**α-3-EtOH**	***β*-3-DMF**	***β*-2-DMF**
formula	$C_{13}H_{10.5}F_3FeO_4P_{0.5}$	$C_{13}H_{10}FeO_4$	$C_{15}H_{17}FeN_{0.5}O_{7.5}Co_{0.75}$	$C_{30}H_{34}Fe_2N_1O_{15}Co_{1.5}$	$C_{15}H_{17}Fe_1N_{0.5}O_{7.5}Ni_{0.75}$	$C_{29}H_{31}Fe_2N_2O_{15}Ni_{1.5}$	$C_{29}H_{31}Fe_2N_2O_{15}Co_{1.5}$
formula wt.	359.05	286.06	424.34	848.68	424.17	847.32	847.66
λ, MoKα	0.71073	0.71073	0.71073	0.71073	0.71073	0.71073	0.71073
crystal system	monoclinic	orthorhombic	orthorhombic	monoclinic	orthorhombic	monoclinic	monoclinic
space group	*C*2/*c*	$C222_1$	*Pnnm*	$P2_1/n$	*Pnnm*	$P2_1/n$	$P2_1/n$
color	orange	orange	pink	pink	green	green	pink
a (Å)	17.325(3)	7.5583(12)	13.596(2)	13.7239(7)	13.532(2)	13.4422(19)	13.5063(10)
b (Å)	10.020(2)	11.1289(18)	14.676(2)	15.0724(8)	14.661(2)	15.265(2)	15.3586(11)
c (Å)	15.361(3)	25.784(4)	17.16(2)	15.8600(8)	16.391(2)	15.858(2)	15.8303(11)
α (deg)	90	90	90	90	90	90	90
β (deg)	109.107(2)	90	90	94.5040(10)	90	94.543(2)	95.849(10)
γ (deg)	90	90	90	90	90	90	90
V (Å^3)	2519.7(9)	2168.8(6)	3424.0(8)	3270.5(3)	3359.2(8)	3243.8(7)	3266.7(4)
T (K)	173(2)	296(2)	173(2)	173(2)	173(2)	173(2)	173(2)
Z	8	8	8	4	8	4	4
ρ_{calc} (g/cm^3)	1.893	1.752	1.646	1.723	1.677	1.735	1.724
refl. collected	11343	11292	8467	29776	28852	20833	29127
independent refl.	3065	2634	4161	7953	4250	5695	7674
R(int)	0.0321	0.0433	0.0479	0.0374	0.0482	0.1359	0.0373
*R*1,*wR*2[$I > 2\sigma(I)$]	0.0295/0.0769	0.0379/0.0868	0.0712/0.1883	0.0396/0.1117	0.0435/0.1139	0.0837/0.2070	0.0536/0.1601
*R*1, *wR*2 (all data)	0.0459/0.0824	0.0496/0.0907	0.1237/0.2043	0.0519/0.1160	0.0635/0.1220	0.1481/0.2278	0.0721/0.1693
G.O.F.	1.095	1.055	1.003	1.114	1.084	0.944	1.136

from a 4:1 ethanol/water solution. The bulk material was confirmed by PXRD to be $[H_2\mathbf{1}\cdot H\mathbf{1}][PF_6]$ (see Supporting Information). Anal. Calcd for $[H_2\mathbf{1}\cdot H\mathbf{1}][PF_6]$, $C_{26}H_{21}O_8PF_6Fe_2$: C, 43.32; H, 3.03; Found C, 43.49; H, 2.95. ^{1}H NMR (300.1 MHz, D_2O): δ = 4.96 (s, 5H), 6.85 (s, 4H); ^{13}C NMR (75.5 MHz, D_2O): δ = 92.06, 89.09, 79.56, 79.45. IR: 3200−2300, 3100, 1735, 1540−1475, 1425, 1281, 1138, 1091, 746, and 514 cm^{-1}. The compound decomposes at 175 °C before melting.

α-$[Co_3(\mathbf{1})_4(H_2O)_2(\mu\text{-}H_2O)_2][NO_3]_2\cdot 4EtOH$, α-2-EtOH. An aqueous solution (3.0 mL) of $[H_2\mathbf{1}\cdot H\mathbf{1}][PF_6]$ (29 mg, 0.068 mmol) and $Co(NO_3)_2\cdot 6H_2O$ (119 mg, 0.41 mmol) was diluted with ethanol (9.0 mL). Within a sealed flask, an ethanol solution (4.0 mL) of pyridine (0.012 mL) was allowed to vapor-diffuse into the reaction mixture, in the dark, at room temperature. Red prism-shaped single crystals of α-$[Co_3(\mathbf{1})_4(H_2O)_2(\mu\text{-}H_2O)_2][NO_3]_2\cdot 4EtOH$ (8.4 mg, 16%), hereafter **α-2-EtOH**, were harvested after about 3 weeks. A single crystal structure was obtained, and the bulk material was confirmed by PXRD to have the same structure. Anal. Calcd for $[Co_3(\mathbf{1})_4(H_2O)_2(\mu\text{-}H_2O)_2][NO_3]_2\cdot 4EtOH$, $C_{60}H_{68}N_2O_{30}Fe_4Co_3$: C, 40.54; H, 3.77; N, 1.69; Found C, 40.38; H, 3.43; N, 1.73.

α-$[Ni_3(\mathbf{1})_4(H_2O)_2(\mu\text{-}H_2O)_2][NO_3]_2\cdot 4EtOH$, α-3-EtOH. An aqueous solution (3.0 mL) of $[H_2\mathbf{1}\cdot H\mathbf{1}][PF_6]$ (37 mg, 0.087 mmol) and $Ni(NO_3)_2\cdot 6H_2O$ (92 mg, 0.32 mmol) was diluted with ethanol (9.0 mL). Within a sealed flask, an ethanol solution (4.0 mL) of triethylamine (0.012 mL) was allowed to vapor-diffuse into the reaction mixture, in the dark, at room temperature. Green prism-shaped single crystals of α-$[Ni_3(\mathbf{1})_4(H_2O)_2(\mu\text{-}H_2O)_2][NO_3]_2\cdot 4EtOH$ (22 mg, 34%), hereafter **α-3-EtOH**, were harvested after about 3 weeks. A single crystal structure was obtained and the bulk material was confirmed by PXRD to have the same structure. Anal. Calcd for $[Ni_3(\mathbf{1})_4(H_2O)_2(\mu\text{-}H_2O)_2][NO_3]_2\cdot 4EtOH$, $C_{60}H_{68}N_2O_{30}Fe_4Ni_3$: C, 40.55; H, 3.77; N, 1.69; Found C, 40.28; H, 3.48; N, 1.56.

***β*-$[Co_3(\mathbf{1})_4(H_2O)_2(\mu\text{-}H_2O)_2][NO_3]_2\cdot 4EtOH$, *β*-2-EtOH.** An aqueous solution (3.0 mL) of $[H_2\mathbf{1}\cdot H\mathbf{1}][PF_6]$ (31 mg, 0.071 mmol) and $Co(NO_3)_2\cdot 6H_2O$ (73 mg, 0.25 mmol) was diluted with ethanol (9.0 mL). Within a sealed flask, an ethanol solution (4.0 mL) of triethylamine (0.012 mL) was allowed to vapor-diffuse into the reaction mixture, in the dark, at room temperature. Red prism-shaped single crystals of *β*-$[Co_3(\mathbf{1})_4(H_2O)_2(\mu\text{-}H_2O)_2]$-$[NO_3]_2\cdot 4EtOH$ (14 mg, 26%), hereafter ***β*-2-EtOH**, were harvested after about 3 weeks. A single crystal structure was obtained, and the bulk material was confirmed by PXRD to have the same structure. Anal. Calcd for $[Co_3(\mathbf{1})_4(H_2O)_2(\mu\text{-}H_2O)_2][NO_3]_2\cdot 4EtOH$, $C_{60}H_{68}N_2O_{30}Fe_4Co_3$: C, 40.54; H, 3.77 ; N, 1.69; Found C, 40.38; H, 3.39; N, 1.79.

***β*-$[Co_3(\mathbf{1})_4(H_2O)_2(\mu\text{-}H_2O)_2][NO_3]_2\cdot 2DMF\cdot 2H_2O$, *β*-2-DMF.** An aqueous solution (2.0 mL) of $[H_2\mathbf{1}\cdot H\mathbf{1}][PF_6]$ (19 mg, 0.045 mmol) and $Co(NO_3)_2\cdot 6H_2O$ (60 mg, 0.21 mmol) was diluted with 10 mL of dimethylformamide. The solution was then placed in a sealed vial and kept at 45 °C for 2 weeks. Red prismatic crystals of *β*-$[Co_3(\mathbf{1})_4(H_2O)_2(\mu\text{-}H_2O)_2][NO_3]_2\cdot 2DMF\cdot 2H_2O$ (5.0 mg, 15%), hereafter ***β*-2-DMF**, were obtained. A single crystal structure was obtained, and the bulk material was by PXRD confirmed to have the same structure. Anal. Calcd for $[Co_3(\mathbf{1})_4(H_2O)_2(\mu\text{-}H_2O)_2]$-$[NO_3]_2\cdot 2DMF\cdot 2H_2O$, $C_{58}H_{62}N_4O_{30}Fe_4Co_3$: C, 40.47; H, 3.64 ; N, 2.92; Found C, 40.56; H, 3.50; N, 2.66.

***β*-$[Ni_3(\mathbf{1})_4(H_2O)_2(\mu\text{-}H_2O)_2][NO_3]_2\cdot 2DMF\cdot 2H_2O$, *β*-3-DMF.** An aqueous solution (2.0 mL) of $[H_2\mathbf{1}\cdot H\mathbf{1}][PF_6]$ (24 mg, 0.045 mmol) and $Ni(NO_3)_2\cdot 6H_2O$ (72 mg, 0.21 mmol) was diluted with 10 mL of dimethylformamide. The solution was then placed in a sealed vial and kept at 45 °C for 2 weeks. Pale yellowish green prismatic crystals of *β*-$[Ni_3(\mathbf{1})_4(H_2O)_2(\mu\text{-}H_2O)_2]$ $[NO_3]_2\cdot 2DMF\cdot 2H_2O$ (12.4 mg, 29%), hereafter ***β*-3-DMF**, were obtained. A single crystal structure was obtained, and the bulk material was confirmed by PXRD to have the same structure. Anal. Calcd for $[Ni_3(\mathbf{1})_4(H_2O)_2(\mu\text{-}H_2O)_2][NO_3]_2\cdot 2DMF\cdot 2H_2O$, $C_{58}H_{62}N_4O_{30}Fe_4Ni_3$: C, 40.49; H, 3.64; N, 2.92; Found C, 40.53; H, 3.60; N, 2.72.

Results and Discussion

Synthesis and Characterization of the Ligand. In 1967, Nesmeyanov reported that the permanganate oxidation of [CpFe(*p*-xylene)][BF_4] yielded a mixture of the metalated dicarboxylic acid $[H_2\mathbf{1}][BF_4]$ and the partially oxidized sandwich compound, [CpFe(*p*-methylbenzoic acid)][BF_4].[37] Working with the $[PF_6]^-$ salt of [CpFe(*p*-xylene)]$^+$, we have been successful in isolating the doubly oxidized terepthalate product in pure form. Our efforts to synthesize the fully protonated $[H_2\mathbf{1}][PF_6]$ form, however, yielded only the monoprotonated zwitterion **H1**, and/or $[H_2\mathbf{1}\cdot H\mathbf{1}][PF_6]$, a 1:1 co-crystal of the doubly

(37) Nesmeyanov, A.; Vol'kenau, N.; Sirotkina, E. *Izvest. Akad. Nauk SSSR* **1967**, *5*, 1170.

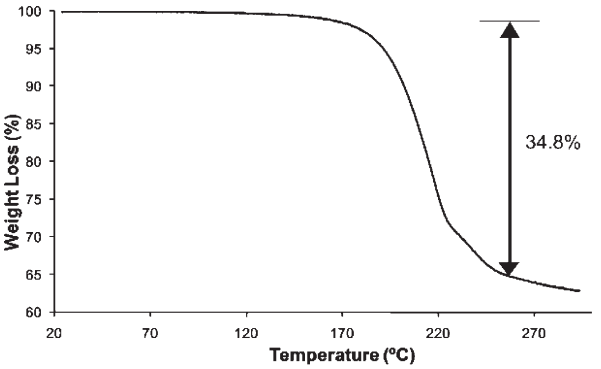

Figure 1. TGA of $[H_2\mathbf{1}\cdot H\mathbf{1}][PF_6]$, illustrating loss of HPF_6 and monodecarboxylation of $[H_2\mathbf{1}]^+$ and H**1** (calc. 32.6%).

protonated $[H_2\mathbf{1}][PF_6]$ and the monoprotonated H**1**, depending on the conditions of the workup. Notably, the reproducible isolation of phase-pure H**1** proved to be elusive, and the ligand was more easily isolated as $[H_2\mathbf{1}\cdot H\mathbf{1}][PF_6]$. It was found that the phase purity of $[H_2\mathbf{1}\cdot H\mathbf{1}][PF_6]$ was essential to ensure reproducible syntheses of the corresponding MOMF materials, and, although the yield of $[H_2\mathbf{1}\cdot H\mathbf{1}][PF_6]$ is modest (35%), the procedure outlined in the experimental section leads to pure $[H_2\mathbf{1}\cdot H\mathbf{1}][PF_6]$, as established by powder X-ray diffraction. Thus, $[H_2\mathbf{1}\cdot H\mathbf{1}][PF_6]$ was fully characterized (X-ray diffraction, elemental analysis, TGA, NMR and IR spectroscopy) and was used in the synthesis of all MOMFs reported herein. The difficulty in isolating pure $[H_2\mathbf{1}][PF_6]$ can likely be attributed to its acidity; η^6-coordination of the electron withdrawing $[CpFe]^+$ moieties is known to considerably enhance the acidity of benzoic acids. For example, the pK_a value of $[CpFe(C_6H_5COOH)][PF_6]$ shows that the metalated species is an order of magnitude more acidic than its parent benzoic acid.[38] In fact, $[CpFe]^+$-metalated benzoic acids like H**1** and $[H_2\mathbf{1}\cdot H\mathbf{1}][PF_6]$ are highly water-soluble compounds, a fact that can be attributed to their charge and/or enhanced acidity. The $[CpFe]^+$ moiety also significantly affects the thermal stability of the acids. According to TGA under N_2 atmosphere (Figure 1), $[H_2\mathbf{1}\cdot H\mathbf{1}][PF_6]$ loses 34.8% of its mass in the temperature range of 170−250 °C, likely attributable to the loss of two molecules of CO_2 and one molecule of HPF_6 per formula unit (32.6% calc.).

Single crystal structures were obtained for both forms of the ligand (Figure 2, Table 1). These are the first reported crystal structures of a benzoic acid moiety that is η^6-coordinated to the $[CpFe]^+$ group, though the Fe−C distances are consistent with other $[CpFe(arene)]^+$ complexes.[39] The crystal structures bear similarity to other organometallic sandwich compounds of carboxylic acids[14,40] in the sense that they form extended H-bonded structures (Figure 2), the details of which are described in the Supporting Information. Of greatest relevance here is the observation that in the crystal structure of zwitterionic H**1**, the ligand reveals a significant out of plane

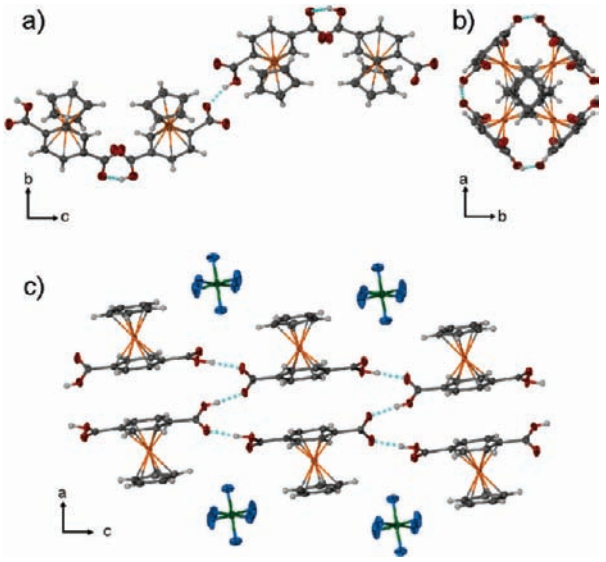

Figure 2. (a) X-ray single crystal structure of H**1** depicting the helical H-bonded chain; (b) the helical H-bonded chain of H**1** as viewed down the *c*-axis; (c) H-bond connectivity observed in the crystal structure of $[H_2\mathbf{1}\cdot H\mathbf{1}][PF_6]$, as viewed down the *b*-axis. For clarity, only one occupied position of the disordered protons is shown. Thermal ellipsoids are shown at 50% probability.

bending of both carboxylate carbon atoms toward the iron metal center such that it deviates significantly from linearity. Instead, the angle defined by the two carboxylate carbons and the arene ring centroid is observed to be 170°. In $[H_2\mathbf{1}\cdot H\mathbf{1}][PF_6]$, however, the same angle measures 178°, and the ligand is essentially linear. Ligand $\mathbf{1}^-$ therefore exhibits a reasonable degree of shape flexibility that can accommodate the optimization of the primary interactions that drive crystal packing (e.g., H-bonds).

MOMFs of $\mathbf{1}^-$. The terephthalate ligand is ubiquitous and important in MOF chemistry,[22−24] and it was of initial interest to examine the feasibility of constructing metal-*organometallic* frameworks (MOMFs) from its $[(\eta^5\text{-Cp})Fe^{II}]^+$-derivatized sandwich compound, $\mathbf{1}^-$. The first 3D framework structures derived from $\mathbf{1}^-$ were from reactions with Co^{II} and Ni^{II} nitrates, outlined in the following sections. Many Co^{II} and Ni^{II} based 1D/2D coordination polymers[41] and 3D frameworks[42] of terephthalate exist for comparison, these polymers

(38) The pK_a of $[CpFe(C_6H_5COOH)]^+$ is 3.05 whereas the pK_a of benzoic acid is 4.2; Nesmeyanov, A. N.; Vol'kenau, N. A.; Sirotkina, E. I. *Russ. Chem. Bull.* **1969**, *18*, 1066.

(39) (a) Hubig, S.; Lindeman, S.; Kochi, J. K. *Coord. Chem. Rev.* **2000**, *200*, 831. (b) Abd-El-Aziz, A.; Bernardin, S. *Coord. Chem. Rev.* **2000**, *203*, 219. (c) Guennec, N.; Moinet, C. *J. Organomet. Chem.* **1995**, *487*, 177.

(40) Braga, D.; Maini, L.; Polito, M.; Tagliavini, E.; Grepioni, F. *Coord. Chem. Rev.* **2003**, *246*, 53–71.

(41) (a) Groeneman, R.; MacGillivray, L.; Atwood, J. *Inorg. Chem.* **1999**, *38*, 208. (b) Go, Y.; Wang, X.; Anokhina, E.; Jacobson, A. *Inorg. Chem.* **2004**, *43*, 5360–5367. (c) For other examples of 1D and 2D Co^{II} terephthalates, see Cambridge Structural Database ref. codes: BAXXAA, BECDOD, BIDVEQ, BOFGOT, HIQQOO, LEZQEN, RAMHES, RAMHES01, RAMHES02, TEWKOW.(d) For other examples of 1D and 2D Ni^{II} terephthalates, see Cambridge Structural Database ref. codes: AGOWUO, AMAPEJ, BIYDUJ, KIVSOY, PIJZAK, SIJNEF, WAQCAS, WEKHOK.

(42) (a) Chun, H.; Jung, H.; Koo, G.; Jeong, H.; Kim, D.-K. *Inorg. Chem.* **2008**, *47*, 5355. (b) Poulsen, R.; Bentien, A.; Christensen, M.; Iversen, B. *Acta Cryst., Sect. B* **2006**, *62*, 245. (c) Clausen, H.; Overgaard, J.; Chen, Y.; Iversen, B. *J. Am. Chem. Soc.* **2008**, *130*, 7988. (d) Zhu, L.-G.; Xiao, H.-P. *Z. Anorg. Allg. Chem.* **2008**, *634*, 845. (e) Wang, Y.-H.; Li, Y.-W.; Chen, W.-L.; Li, Y.-G.; Wang, E.-B. *J. Mol. Struct.* **2008**, *877*, 56. (f) Fang, Q.-R.; Shi, X.; Xin, M.-H.; Wu, G.; Tian, G.; Zhu, G.-S.; Li, Y.-F.; Ye, L.; Wang, C.-L.; Zhang, Z.-D.; Tang, L.-L.; Qiu, S. *Chem. J. Chin. Univ.* **2003**, *24*, 980. (g) Liu, G.-X.; Xu, H.; Ren, X.-M. *Z. Anorg. Allg. Chem.* **2008**, *634*, 927. (h) Li, X.-H.; Yang, S.-Z.; Xiao, H.-P. *Cryst. Growth Des.* **2006**, *6*, 2392. (i) Tao, J.; Tong, M.-L.; Chen, X.-M. *J. Chem. Soc., Dalton Trans.* **2000**, 3669. (j) Fu, Z.-Y.; Wu, X.-T.; Dai, J.-C.; Hu, S.-M.; Du, W.-X.; Zhang, H.-H.; Sun, R.-Q. *Eur. J. Inorg. Chem.* **2002**, 2730. (k) Yang, S.-Y.; Long, L.-S.; Tao, J.; Huang, R.-B.; Zheng, L.-S.; Ng, S. *Acta Crystallogr.* **2003**, *E59*, m454.

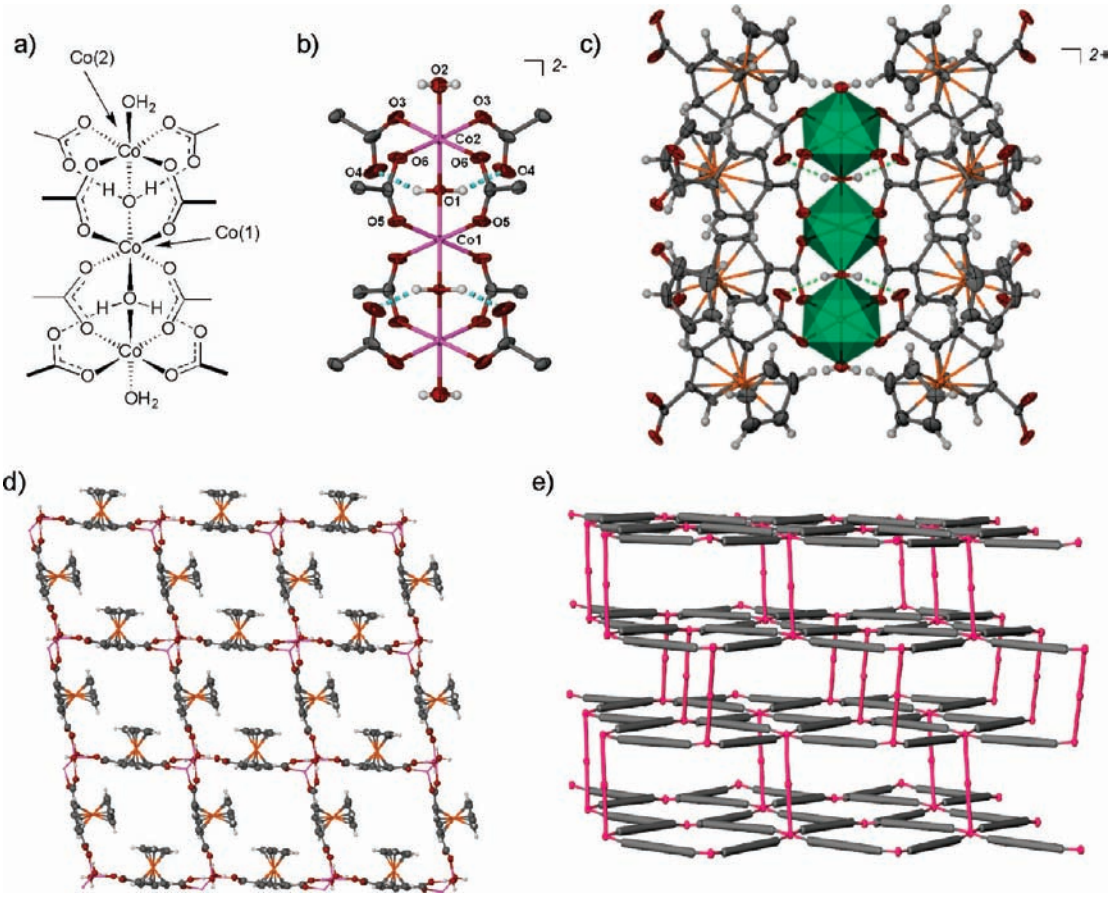

Figure 3. Schematic diagram (a), thermal ellipsoid plot (b,c), and polyhedral representation (c) of the trinuclear cluster observed in the X-ray crystal structure of α-[Co_3(**1**)$_4$(H_2O)$_2$(μ-H_2O)$_2$][NO_3]$_2$·4EtOH, **α-2-EtOH**; d) the 2D square grid network of **α-2-EtOH**, illustrating the in-in-out-out arrangement of the $[CpFe]^+$ moieties around the squares; (e) the 3D body centered tetragonal network topology of **α-2-EtOH** (magenta nodes represent cobalt metal centers and gray struts represent the $\mathbf{1}^-$ ligands that connect the square grids).

occasionally being sustained by additional chelating or bridging ligands. Some of these materials exhibit permanent porosity and are of interest for gas storage and/or related applications,[42a] whereas some Co^{II}-based terephthlates are of interest in relation to their magnetic properties.[42b,42c] An organometallic form of terephthalate such as $\mathbf{1}^-$ also offers opportunities in these directions and provides additional opportunities related to the presence of the $[(\eta^5\text{-Cp})Fe^{II}]^+$ moieties, as outlined in the introduction. Opportunities that take advantage of the photochemical properties of $\mathbf{1}^-$ will form the basis of further study.

"In-in-out-out" Frameworks. Reaction of [H_2**1**·H**1**][PF_6] and $Co(NO_3)_2\cdot 6H_2O$ in ethanol/water in the presence of pyridine vapor yielded large red prisms of α-[Co_3(**1**)$_4$(H_2O)$_2$(μ-H_2O)$_2$][NO_3]$_2$·4EtOH, **α-2-EtOH**,[43] which were analyzed by single crystal X-ray diffraction. The structure consists of clusters of three linearly connected, octahedrally coordinated Co(II) ions propagated by metalated terephthalate ligands ($\mathbf{1}^-$) as bridges to form a 3D framework. The trinuclear cluster is essentially a short rod of three corner shared Co^{II} octahedra as shown in Figure 3a–c. Notably, despite the considerable attention paid to metal carboxylate based materials in recent years, the trinuclear clusters observed in **α-2-EtOH** constitute new structural/secondary building units (SBUs)[2a] in MOF chemistry. Several Co^{II} terephthlate coordination polymers do, however, adopt similar trinuclear clusters.[42a–42c,44] The trinuclear clusters of **α-2-EtOH** are located on crystallographic 2/*m* (C_{2h}) positions such that there are two unique Co(II) ions by symmetry. Co2, located at either end of the three-metal cluster, is coordinated in the equatorial positions by the carboxylate oxygens of four molecules of $\mathbf{1}^-$, and in the axial positions by water molecules, one that is terminal (Co2–O2 = 2.080(6) Å) and another that bridges to the central ion, Co1 (Co2–O1 = 2.114(5) Å). Of the four carboxylates surrounding Co2, two are monodentate, arranged in a cisoid fashion (Co2–O3 = 2.084(4) Å), and two serve as bridges, connecting Co2 to the central Co1 atom in a cisoidal, syn-syn bonding mode (Co2–O6 = 2.052(4) Å). Thus, the central Co1 ion is coordinated in the axial positions by two bridging water molecules (Co1–O1 = 2.084(4) Å) and in the equatorial positions by the carboxylate oxygens atoms of four symmetry equivalent molecules of $\mathbf{1}^-$ (Co1–O5 = 2.080(4) Å), each of which is bridging to an adjacent Co2 ion. The cluster is further supported by four strong

(43) In keeping with the practice of defining appropriate acronyms for new framework materials, we alternatively name the frameworks of α/β-[Co_3(**1**)$_4$(H_2O)$_2$(μ-H_2O)$_2$][NO_3]$_2$ and α/β-[Ni_3(**1**)$_4$(H_2O)$_2$(μ-H_2O)$_2$][NO_3]$_2$ as α/β-**GU-MOMF-1** and α/β-**GU-MOMF-2**, respectively.

(44) (a) Zhang, L.-J.; Zhao, X.-L.; Cheng, P.; Xu, J.-Q.; Tang, X.; Cui, X.-B.; Xu, W.; Wang, T.-G. *Bull. Chem. Soc. Jpn.* **2003**, *76*, 1179. (b) Fang, Q.-R.; Shi, X.; Xin, M.-H.; Wu, G.; Tian, G.; Zhu, G.-S.; Li, Y.-F.; Ye, L.; Wang, C.-L.; Zhang, Z.-D.; Tang, L.-L.; Qiu, S. *Chem. J. Chin. Univ.* **2003**, *24*, 980.

O−H···O hydrogen bonds between the two bridging water molecules and the monodentate carboxylate ligands (O(H)···O = 2.598(5) Å).

The result of the trinuclear coordination cluster is that each of the Co2-based octahedra are propagated into a 2D square grid network in the (100) planes by the action of $\mathbf{1}^-$ ligands as linear connectors. Though the $\mathbf{1}^-$ ligands serve as linear connectors they are in fact slightly bent; as observed in the crystal structure of H**1**, the angle defined by the two carboxylate carbons of $\mathbf{1}^-$ and the arene ring centroid is observed to be 171.5°. As the Co2 ions are also connected via Co1 centers within the metal-carboxylate clusters, so, too, are the square grids interconnected in the third dimension, such that the overall framework topology can be considered a body centered, tetragonal net. It can be described by square grid nets that are connected alternately in an up−down fashion along the nodes of the grid, which are defined by the trinuclear clusters. The $[CpFe]^+$ moieties in the square grids are oriented in such a fashion that in each square, two of these moieties are found adjacent to each other in an alternating "in-in-out-out" pattern as shown in Figure 3d. The $[CpFe]^+$ moieties partially fill the squares, thereby preventing interpenetration, but leaving about 4.6 × 4.6 Å (accounting for van der Waals radii) square cavities that are each filled with two disordered ethanol molecules.

Were the $[CpFe]^+$ moieties not attached to the terephthalate ligands the overall framework would hold a two-minus charge per formula unit (Figure 3b). It is perhaps not surprising, therefore, that the trinuclear SBU found in **α-2-EtOH** is unobserved elsewhere in MOF chemistry, as it would require that the structure incorporate a non-coordinating countercation. For instance, the related trinuclear Co^{II} terephthalate cluster found in $[Et_2NH_2]_2[Co_3(1,4\text{-bdc})_4]\cdot 3DEF$ (DEF = diethylformamide) incorporates two triethylammonium ions per formula unit, which are only made available by the hydrolysis of the DEF solvent under solvothermal conditions.[42b,42c] In **α-2-EtOH**, the presence of the positively charged $[CpFe]^+$ moieties dons the framework with an overall two-plus charge per formula unit. Accordingly, two non-coordinating NO_3^- ions (per formula unit) are located in the structure and are strongly associated with the terminally coordinated H_2O molecules via hydrogen bonds, thus preventing them from filling the cavities of the squares grids. The ethanol solvent molecules and nitrate anions within the cavities of **α-2-EtOH** were found to be highly disordered. Thus, the SQUEEZE subroutine of PLATON was employed to model these disordered species. SQUEEZE attributes 150 e^- (per formula unit) to the disordered species, which agrees well with that calculated for four ethanol molecules and two nitrate anions (156 e^-). TGA and elemental analysis of **α-2-EtOH** further supports the formulation (vide infra).

Reaction of $[H_2\mathbf{1}\cdot H\mathbf{1}][PF_6]$ and $Ni(NO_3)_2\cdot 6H_2O$ in ethanol/water in the presence of pyridine vapor gave large green crystals of α-$[Ni_3(\mathbf{1})_4(H_2O)_2(\mu\text{-}H_2O)_2][NO_3]_2\cdot$ 4EtOH, **α-3-EtOH**,[43] in modest yield. Single crystal X-ray diffraction studies showed **α-3-EtOH** to be entirely isostructural to **α-2-EtOH**. In fact, about the only notable differences between **α-2-EtOH** and **α-3-EtOH** are the slightly shorter metal oxygen bond lengths

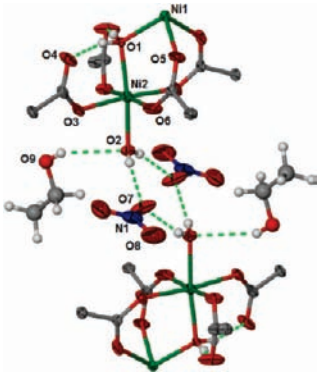

Figure 4. Hydrogen bonding interactions between terminal waters of the trinuclear clusters, lattice nitrate anions, and included ethanol guests observed in the single crystal structure of **α-3-EtOH**. Only the major occupancy portions of disordered nitrate and ethanol species are shown.

(Ni1−O1 = 2.037(2)Å, Ni1−O5 = 2.033(3) Å, Ni2−O1 = 2.065(3) Å, Ni2−O2 = 2.050(3) Å, Ni2−O3 = 2.050(2) Å, Ni−O6 = 2.014(2) Å) and the consequently smaller unit cell volume in the latter (3434 $Å^3$ and 3359 $Å^3$, respectively, at 173(2) K). The shorter metal oxygen distances and smaller unit cell volume imply that the dimensions of the ethanol-occupied square cavities defined by the framework of **α-3** are slightly smaller than those of **α-2**. Interestingly, the ethanol solvent molecules and the nitrate counteranions are more ordered in **α-3-EtOH** than in **α-2-EtOH**, a fact that no doubt can be attributed to the tighter fit of these species within the slightly smaller framework of **α-3**. Thus, these species were accurately modeled in the refinement of **α-3-EtOH**, and the formulation of four ethanols and two nitrate anions per formula unit is established unequivocally. Moreover, the non-covalent associations between the host framework and the included solvents and nitrate anions are discernible in **α-3-EtOH** (Figure 4). Each terminal water molecule of the trinuclear clusters forms strong hydrogen bonds to two nitrate anions (O2-(H)···O7 = 2.725(6) Å) and the nitrates serve to form H-bonded bridges between the trinuclear clusters of adjacent square grids. The terminal water molecules also serve as hydrogen bond acceptors, participating in a hydrogen bond with one of the two symmetry-independent ethanol molecules (O9(H)···O2 = 3.133(9) Å). The remaining symmetry-independent ethanol molecule seemingly does not participate in any hydrogen bond interactions. Lastly, to validate the results obtained in the SQUEEZE refinement of **α-2-EtOH**, the SQUEEZE subroutine of PLATON was employed, in an alternative refinement (not reported), to model the electron density of the ethanol molecules and nitrate anions of **α-3-EtOH**. SQUEEZE attributed 156 e^- (per formula unit) to these species, agreeing exactly with the calculated value for four ethanol molecules and two nitrate anions. TGA and elemental analysis of **α-3-EtOH** also supports its formulation (vide infra).

"In-out-in-out" frameworks. Reaction of $[H_2\mathbf{1}\cdot H\mathbf{1}][PF_6]$ and $Co(NO_3)_2\cdot 6H_2O$ in ethanol/water in the presence of triethylamine vapor (vs pyridine used in the synthesis of **α-2-EtOH)** gives large red prisms of β-$[Co_3(\mathbf{1})_4(H_2O)_2(\mu\text{-}H_2O)_2][NO_3]_2\cdot 4EtOH$, hereafter

***β*-2-EtOH**. Remarkably, ***β*-2-EtOH** is a polymorph[45] of **α-2-EtOH**, possessing the same molecular formula, the same trinuclear coordination clusters (Figure 5a,b), the same body centered tetragonal network structure, and the same number of included ethanol molecules as **α-2-EtOH** (vide infra). The primary difference between ***β*-2-EtOH** and **α-2-EtOH** lies in the orientation of the $[CpFe]^+$ moieties within the 2D square grid substructure of the 3D framework. That is, the $[CpFe]^+$ moieties in ***β*-2-EtOH** are oriented in such a fashion that within each square, they are found facing each other in an alternating "in-out-in-out" pattern (Figure 5c), in obvious contrast to the "in-in-out-out" arrangement found in **α-2-EtOH** (Figure 3d). The result is a distorted, wave-like square grid substructure that is very similar to the square grid substructure observed recently in $[Co_2(1,4\text{-bdc})_2$(diazobycyclo[2.2.2]octane)].[42d] This alternative arrangement of the $[CpFe]^+$ moieties also leads to a loss of mirror symmetry and a distortion of the trinuclear clusters such that they lie on an inversion center in ***β*-2-EtOH** (vs $2/m$ (i.e., C_{2v}) symmetry in **α-2-EtOH**). The square grids in the ***β*-2-EtOH** polymorph have cavities of about 3.6 × 4.4 Å, accounting for van der Waals radii. The cobalt to oxygen distances in ***β*-2-EtOH**, however, are not appreciably different (< 0.04 Å) from those observed in α-2-EtOH (Co2−O1 = 2.123(2) Å, Co2−O2 = 2.071(2) Å, Co2−O3 = 2.116(2) Å, Co2−O6 = 2.056 (2) Å, Co2−O7 = 2.081(2) Å, Co2−O9 = 2.091(2) Å, Co1−O5= 2.077(2) Å, Co1−O10 = 2.058(2) Å). Relative to the α-2 framework, the different orientations of the $[CpFe]^+$ moieties around the cobalt centers in the ***β*-2** framework are accommodated only by subtle differences in many of the torsion and bond angles throughout the framework. For example, the $\mathbf{1}^-$ ligands are only slightly more bent in ***β*-2-EtOH** as compared to **α-2-EtOH**, with the angles between the carboxylate carbons of the $\mathbf{1}^-$ ligands and the arene ring centroids measuring 167.9° and 170.1° in ***β*-2-EtOH** (vs 171.5° in **α-2-EtOH**).

Interestingly, ***β*-2-EtOH** has a unit cell volume that is ∼5% smaller than its **α-2-EtOH** polymorph (3424 $Å^3$ vs 3270 $Å^3$, respectively), with the largest dimensional difference being along the *c* axis. Though the included solvent molecules and nitrate anions are highly disordered in ***β*-2-EtOH** and could not adequately be resolved, SQUEEZE analysis estimated that 135 e^- per formula unit should be attributed to these species. Though this value falls short of what one expects for exactly four ethanol molecules per formula unit (156 e^-, including nitrate anions), we note that single crystals of ***β*-2-EtOH** were consistently twinned, and the SQUEEZE results could be affected by refining upon data derived from a twinned single crystal sample. Moreover, the ascribed composition of four ethanols per formula unit is supported by both TGA (vide infra) and elemental analysis.

As the only difference between the synthesis of **α-2-EtOH** and ***β*-2-EtOH** was in the base employed (pyridine or triethylamine, respectively), it was anticipated that the use of triethylamine in the reaction of $[H_2\mathbf{1}\cdot\mathbf{H1}][PF_6]$ and $Ni(NO_3)_2\cdot 6H_2O$ in ethanol/water would yield β-$[Ni_3(\mathbf{1})_4(H_2O)_2(\mu\text{-}H_2O)_2][NO_3]_2\cdot 4$EtOH, ***β*-3-EtOH**, a polymorph of **α-3-EtOH**. Surprisingly, crystals of ***β*-3-EtOH** were not isolated under any conditions. Instead, all attempts at the synthesis of ***β*-3-EtOH** yielded exclusively **α-3-EtOH** according to single crystal and powder X-ray diffraction. The ***β*-3** framework was successfully obtained, however, by the reaction of $[H_2\mathbf{1}\cdot\mathbf{H1}][PF_6]$ and $Ni(NO_3)_2\cdot 6H_2O$ in a DMF/water solution at 45 °C. The resulting green prisms of β-$[Ni_3(\mathbf{1})_4(H_2O)_2(\mu\text{-}H_2O)_2]$-$[NO_3]_2\cdot[DMF]_2[H_2O]_2$, ***β*-3-DMF**, formally a pseudopolymorph[46] of the hypothetical ***β*-3-EtOH**, were found by single crystal X-ray diffraction to possess a framework that was isostructural to ***β*-2-EtOH**. The included DMF and water solvent molecules were found to be highly disordered and could not be adequately modeled. SQUEEZE was once again employed to model the disordered water and DMF molecules, ascribing 99 e^- per formula unit to these species. This number compares favorably to that calculated for two DMF and two water molecules (100 e^-). TGA and elemental analysis further support the formulation (vide infra).

Under the same reaction conditions that resulted in ***β*-3-DMF**, $[H_2\mathbf{1}\cdot\mathbf{H1}][PF_6]$ and $Co(NO_3)_2\cdot 6H_2O$ were

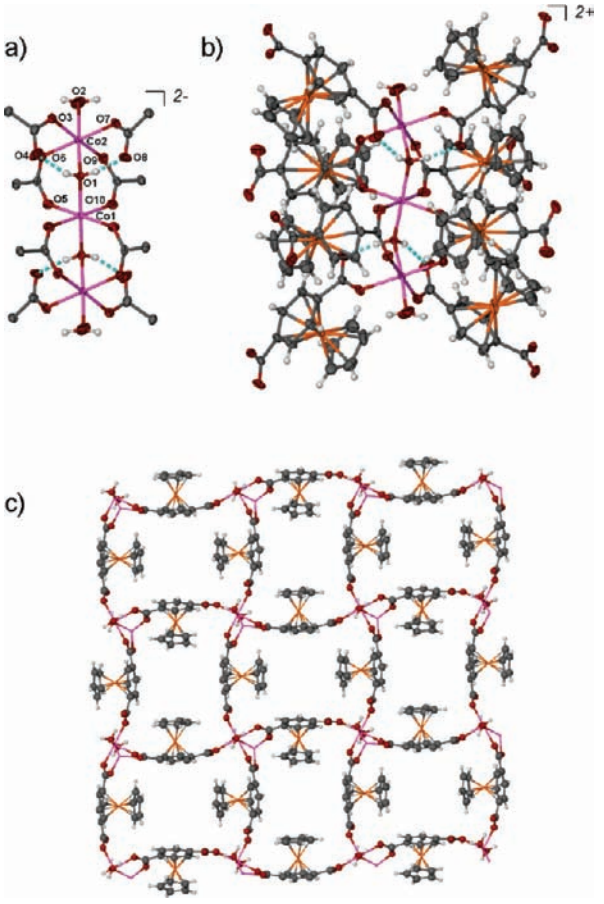

Figure 5. Thermal ellipsoid plot (a, b) of the trinuclear cluster observed in the X-ray crystal structure of β-$[Co_3(\mathbf{1})_4(H_2O)_2(\mu\text{-}H_2O)_2][NO_3]_2\cdot 4$-EtOH, ***β*-2-EtOH**; (c) the 2D square grid network of ***β*-2-EtOH**, illustrating the "in-out-in-out" arrangement of the $[CpFe]^+$ moieties around the squares.

(45) (a) Bernstein, J. *Polymorphism in Molecular Crystals*; Oxford University Press: Oxford, U.K., 2002.(b) Robin, A.; Fromm, K. *Coord. Chem. Rev*. **2006**, *250*, 2127.

(46) Nangia, A.; Desiraju, G. *Chem. Commun*. **1999**, *7*, 605.

reacted to yield large red prismatic crystals of β-$[Co_3(\mathbf{1})_4(H_2O)_2(\mu\text{-}H_2O)_2][NO_3]_2\cdot[DMF]_2[H_2O]_2$, ***β*-2-DMF**. Single crystal X-ray diffraction studies showed that the MOMF of ***β*-2-DMF** is isostructural to the frameworks of ***β*-2-EtOH** and ***β*-3-DMF**. ***β*-2-DMF** is in fact a pseudopolymorph of ***β*-2-EtOH**, being different only with respect to its included solvent. SQUEEZE was again used to model disordered water and DMF molecules and indicated that 98.5 e^- per formula unit could be ascribed to these species. The number agrees well with the number of electrons expected for two DMF and two water molecules (100 e^-). TGA and elemental analysis of ***β*-2-DMF** also support the formulation.

Polymorphism. An important ramification of the polymorphism (and pseudopolymorphism) in the **α-2/3** and ***β*-2/3** MOMF frameworks of $\mathbf{1}^-$ (i.e., the "in-in-out-out" and "in-out-in-out" arrangement of the ligands) is the difference in the shape of the spaces that the frameworks afford for their included guests. In the **α** frameworks, the "in-in-out-out" arrangements of the $[CpFe]^+$ moieties in the squares of the 2D grids defines the cavities as being in the *corners* of the squares. As the 2D square grids in the framework are related by inversion centers between the layers, the cavities defined by the grids reside in opposite corners of the squares along the *a*-axis in the crystal (Figure 6a). The solvent-occupied cavities of the **α** frameworks are therefore isolated from one other. In the ***β*** frameworks, however, the "in-out-in-out" arrangements of the $[CpFe]^+$ moieties within the squares of the 2D grids define the cavities as being in the *centers* of the squares. As with the **α** frameworks, the square grids of the ***β*** frameworks are related by inversion centers between the layers, but in the ***β*** structures the cavities are superimposed upon one another along the *a*-axis, giving rise to one-dimensional solvent-occupied channels (Figure 6b).

Thus, it can be recognized that it is the presence of the $[CpFe]^+$ moieties that gives rise to the most salient features (polymorphism and cavity vs channel structure) of these MOMFs, **α-2/3** and ***β*-2/3**. Indeed, coordination of the $[CpFe]^+$ group to one arene face of the terephthalate moiety differentiates the two faces of the ligand, giving rise to the possibility of isomerism in the decoration of the square grids—the "in-in-out-out" form and the "in-out-in-out" form in this pair of polymorphs. Though other arrangements are conceivable, we think it unlikely, on steric grounds, that one could observe the alternative "all-in" or "in-in-in-out" type of arrangements, since it does not seem possible for the square cavities to accommodate more than two $[CpFe]^+$ moieties. Furthermore, it should be possible to systematically modify the steric demands of the organometallic moiety (e.g., $[(\eta^5\text{-}C_5Me_5)Fe^{II}]^+$ vs $[(\eta^5\text{-}C_5H_5)Fe^{II}]^+$, etc.) to frustrate the square grid arrangement such that an alternative framework structure would be inevitable. Ultimately, we feel such strategies could be beneficial in the synthesis of new framework architectures, particularly those that might be considered rare or so-called non-"default"[30] structures.

(47) (a) Kitaigorodsky, A. I. *Molecular Crystals and Molecules*; Academic Press: New York, 1973.(b) Burger, A.; Ramberger, R. *Mikrochim. Acta* **1979**, *2*, 273.

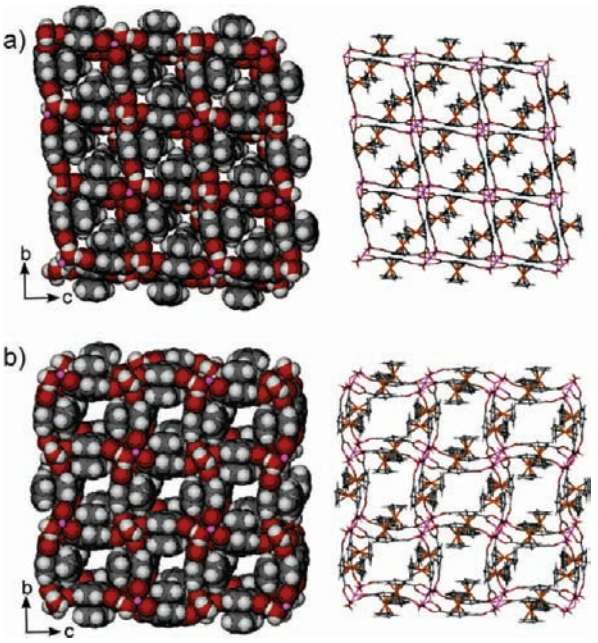

Figure 6. (a) View of **α-2** down the *a*-axis; (b) the channels in ***β*-2** as viewed down the *a*-axis. Nitrate counterions and included solvents have been removed for clarity.

Finally, it is difficult to establish the relative thermodynamic stabilities of the polymorphic **α** and ***β*** materials. By the density rule,[47] one might expect the ***β*** frameworks to be more thermodynamically stable than the **α** forms, as the ***β*** structures are about 3−5% smaller in volume than the **α** structures. As a direct comparison, ***β*-2-EtOH** is apparently more dense than its **α-2-EtOH** polymorph (ρ_{calc} = 1.723 g/cm^{-3} and 1.646 g/cm^{-3}, respectively, at 173(2)K). It should be noted, however, that while we have defined the formula of ***β*-2-EtOH** to contain exactly four ethanol molecules per formula unit on the basis of TGA and elemental analysis data, the SQUEEZE analysis suggested slightly less than four ethanols. One can therefore not formally rule out a non-stoichiometric quantity of ethanol molecules because of a possible incommensurate relationship between the ethanols in the channels and the ***β*-2** framework. Unfortunately, experimental determination of the densities of these materials is complicated by solvent loss, as is differential scanning calorimtery. Another consideration is the fact that the syntheses of ***β*-2-DMF** and ***β*-3-DMF** are performed at 45 °C whereas **α-2-EtOH** and **α-3-EtOH** are synthesized at room temperature. Though this fact might seem to suggest that the ***β*** frameworks are the more thermodynamically stable, experiments have shown that **α-3-EtOH** is obtained even when the synthesis of performed at 120 °C.

Bulk Characterization and Desolvated Frameworks. The phase purity of bulk samples of **α-2-EtOH**, **α-3-EtOH**, ***β*-2-EtOH**, ***β*-2-DMF**, and ***β*-3-DMF** were investigated by powder X-ray diffraction (PXRD) at ambient temperature (Figure 7). The experimentally obtained powder patterns showed excellent agreement with the calculated powder patterns derived from the single crystal structures at 173(2) K, accounting for differences in the sample temperatures. It is difficult, however, to unequivocally establish the phase purity of the **α-2-EtOH** and ***β*-2-EtOH** polymorphs. Though the calculated powder

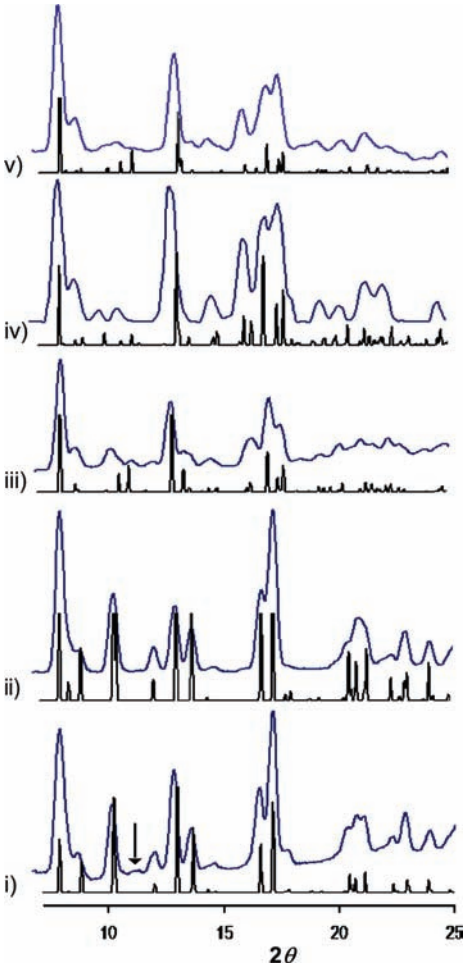

Figure 7. Calculated (black) and experimental (blue) powder patterns of (i) **α-2-EtOH** and (ii) **α-3-EtOH**, (iii) ***β*-2-EtOH**, (iv) ***β*-2-DMF**, and (v) ***β*-3-DMF**. The intensities of some peaks in the calculated patterns have been truncated for clarity.

patterns of these two materials exhibit obvious differences, the breadth of the peaks of the observed patterns makes it difficult to clearly discern these differences experimentally. Nonetheless, the experimental PXRD patterns of **α-2-EtOH** and ***β*-2-EtOH** reproducibly reveal subtle, though significant, characteristic differences in their relative peak intensities and positions. It can therefore be concluded that the **α-2-EtOH** and ***β*-2-EtOH** samples are *mostly* phase-pure. It is likely, however, that **α-2-EtOH** is slightly contaminated by ***β*-2-EtOH**. For instance, at ~11.2° in the diffractogram of **α-2-EtOH**, where there should be no peaks, the (002) reflection of ***β*-2-EtOH** seemingly appears as a small, broad peak (indicated by an arrow in Figure 7). Importantly, the observed PXRD pattern of **α-3-EtOH** establishes its phase purity, noticeably lacking any peak that might be exclusively attributed to a hypothetical ***β*-3-EtOH**. That the observed pattern of **α-2-EtOH** is almost identical to **α-3-EtOH**, which is phase pure, further supports the contention that bulk **α-2-EtOH** is indeed *mostly* phase pure. The PXRD patterns of ***β*-2-DMF** and ***β*-3-DMF** reveal their phase purity.

α-2-EtOH, **α-3-EtOH**, ***β*-2-EtOH**, ***β*-2-DMF**, and ***β*-3-DMF** were subjected to TGA under nitrogen atmosphere to investigate the thermal stability of the solvated

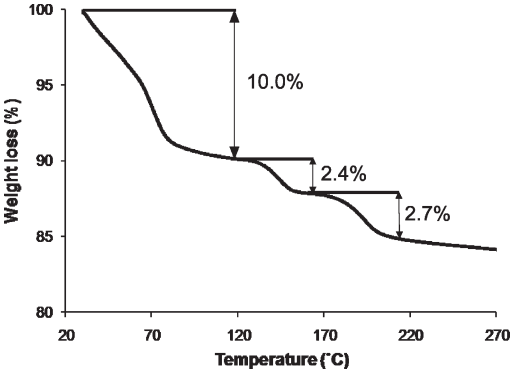

Figure 8. TGA of **α-2-EtOH** under N_2 at a heating rate of 3 °C/min.

materials. The TGA traces of all of these samples have nearly identical characteristics. The TGA trace of **α-2-EtOH** is depicted in Figure 8 whereas the TGA traces of the remaining materials are provided as Supporting Information. For all compounds the total observed mass losses between room temperature and approximately 220 °C agree well with what one expects for the loss of all of the included solvents and coordinated water molecules, the total expected mass losses being 15.1% for **α-2-EtOH**, **α-3-EtOH**, and ***β*-2-EtOH** and 15.0% for ***β*-2-DMF** and ***β*-3-DMF**. The included solvent molecules are lost in a first step (10.9% calc.) below 120 °C, as confirmed by ^{1}H NMR spectroscopy, followed by the loss of the coordinated waters (4.2% calc.), occasionally in two distinct steps, ultimately yielding, at around 220 °C, dark colored, sparingly soluble, amorphous (vide infra) products. Thus, the ethanol and DMF-free apohosts of composition $[Co_3(\mathbf{1})_4(H_2O)_2(\mu\text{-}H_2O)_2][NO_3]_2$ and $[Ni_3(\mathbf{1})_4(H_2O)_2(\mu\text{-}H_2O)_2][NO_3]_2$ have been isolated by heating the samples under N_2 to 90 °C. It is interesting to note that, up to 270 °C, there is no mass loss from the framework materials of $\mathbf{1}^-$ that can be attributed to CO_2, whereas the $[H\mathbf{1}\cdot H_2\mathbf{1}][PF_6]$ starting material loses 2 equiv CO_2 and 1 equiv of HPF_6 from ~175−250 °C. To further establish the thermal stability of the $\mathbf{1}^-$ ligands in these frameworks at elevated temperatures, a sample of **α-2-EtOH** was heated to 180 °C under a nitrogen atmosphere, with its corresponding mass loss being monitored by TGA. The resulting material, having lost exactly 4 equiv of ethanol and exactly two of its four coordinated water molecules (presumably the terminal ones), was completely dissolved in DCl and examined by ^{1}H NMR spectroscopy using *p*-toluenesulfonic acid monohydrate as an internal concentration standard. The spectrum revealed that none of the ligand had decomposed during this treatment. Thus, the material $[Co_3(\mathbf{1})_4(H_2O)_2][NO_3]_2$ (lacking two, presumably terminal, water ligands) can also be isolated. **α-3-EtOH**, ***β*-2-EtOH**, ***β*-2-DMF**, and ***β*-3-DMF** presumably behave similarly as their TGA traces are very similar. Another sample of **α**-2-EtOH, heated to 220 °C and having lost all of its included ethanol and coordinated water molecules, proved to be mostly insoluble in DCl.

To monitor the structure of the MOMF materials as a function of their desolvation, polymorphic **α-2-EtOH** and ***β*-2-EtOH** were analyzed by variable temperature PXRD, and the resulting diffractograms are shown in Figure 9. Of particular interest was the following: (i) whether and to

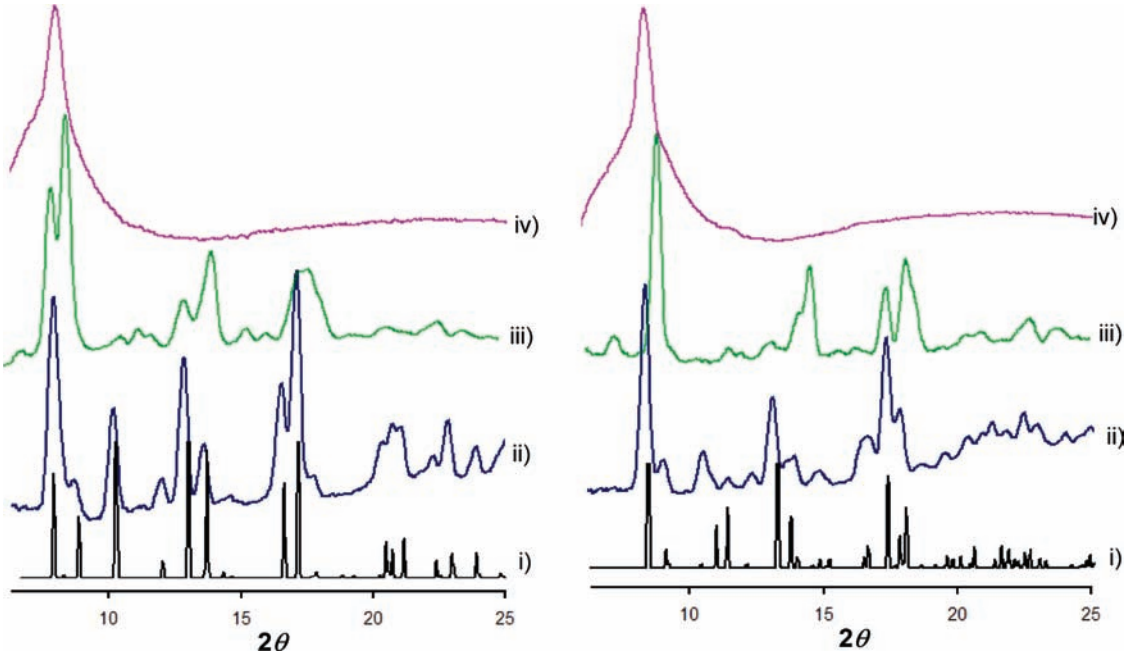

Figure 9. Calculated (i) and experimental (ii) PXRD patterns of **α-2-EtOH** (left) and ***β*-2-EtOH** (right); (iii) ***γ*-2** (left) and ***δ*-2** (right) after heating **α-2-EtOH** and ***β*-2-EtOH**, respectively, to 90 °C under N2; (iv) after heating to 250 °C.

what extent the materials retain their structure upon solvent loss, (ii) whether ethanol-free forms of **α-2-EtOH** and ***β*-2-EtOH**, both having the composition $[Co_3(\mathbf{1})_4(H_2O)_2(\mu\text{-}H_2O)_2][NO_3]_2$, are also polymorphic. Samples of **α-2-EtOH** and ***β*-2-EtOH** were placed in open-ended capillaries, mounted on the powder diffractometer and heated to 90 °C under a constant flow of dry N_2 for 2 h. ^{1}H NMR spectroscopy of the resulting digested materials established the complete loss of included ethanols under these conditions. The PXRD patterns of the still-crystalline, ethanol-free apohosts were both found to be different from their fully solvated forms, implying that loss of ethanol is accompanied by a significant structural change. Moreover, the powder patterns of the ethanol-free apohosts are significantly different from one another, establishing that the apohost of **α-2-EtOH**, hereafter ***γ*-2**, and the apohost of ***β*-2-EtOH**, hereafter ***δ*-2**, are polymorphic forms of the composition $[Co_3(\mathbf{1})_4(H_2O)_2(\mu\text{-}H_2O)_2][NO_3]_2$. Importantly, therefore, ***γ*-2** and ***δ*-2** retain at least some of the structural features of their original, fully solvated forms. It is likely, in fact, that the "in-in-out-out" and "in-out-in-out" ligand arrangements are retained upon desolvation, supporting the contention that the square grid type of connectivity within the frameworks is also retained. Unfortunately, the poor resolution of the powder patterns prohibited indexing and unit cell determinations of ***γ*-2** and ***δ*-2**. Upon further heating under N_2, so as to remove all coordinated water molecules (> 220 °C), both ***γ*-2** and ***δ*-2** lose their crystallinity (Figure 9d).

α-3-EtOH and ***β*-3-DMF** were also analyzed by variable temperature PXRD (see Supporting Information). The fully solvated forms of **3**, namely **α-3-EtOH** and ***β*-3-DMF**, are not formally polymorphic; they are pseudopolymorphic. Upon desolvation, however, the ethanol and DMF-free forms of **α-3-EtOH** and ***β*-3-DMF**, respectively, give different polymorphic forms of $[Ni_3(\mathbf{1})_4(H_2O)_2(\mu\text{-}H_2O)_2][NO_3]_2$, ***γ*-3** and ***δ*-3**, respectively. Notably, the PXRD patterns of ***γ*-3** and ***δ*-3** bear a strong resemblance to the PXRD patterns of ***γ*-2** and ***δ*-2**.

Though the loss of ethanol or DMF from **α-2-EtOH**, ***β*-2-EtOH**, **α-3-EtOH**, and/or ***β*-3-DMF** was accompanied by a change in structure, it was nonetheless of interest to determine whether the resulting ***γ*-2**, ***δ*-2**, ***γ*-3**, or ***δ*-3** apohosts sustained permanent porosity. N_2 sorption analysis of ***γ*-2**, ***δ*-2**, ***γ*-3**, and ***δ*-3** at 77 K revealed that the materials were not microporous.

Selective Guest Absorption. Though apohosts ***γ*-2**, ***δ*-2**, ***γ*-3**, and ***δ*-3** do not exhibit permanent porosity, they quickly take up atmospheric water and/or certain alcohols when exposed to their vapors. To investigate whether these materials are capable of selective absorption, and to determine whether polymorphic framework structures might significantly influence such selectivity, ***γ*-3** and ***δ*-3** were studied with respect to their water and alcohol absorption properties. ***γ*-3** and ***δ*-3** were chosen in preference to ***γ*-2** and ***δ*-2** as they were derived from **α-3-EtOH** and ***β*-3-DMF**, respectively, each of which was unequivocally established to be phase pure (vide supra). ***γ*-3** absorbs up to 5.9 (~6) equiv of water in as little as 10 min at ambient conditions (room temperature, < 50% relative humidity), as determined by TGA. Notably, *γ*-**3** deliquesces at high humidity and, although it is soluble in water, it is generally insoluble in alcohols and most organic solvents (e.g., $CHCl_3$, DMF, CH_2Cl_2, acetonitrile, etc.). As it is unclear whether the framework of the water solvated material has the structure of **α-3**, ***γ*-3**, or an as yet unknown structure, it will simply be referred to as $\mathbf{3}\cdot 6H_2O$. The absorption of alcohol vapors by ***γ*-3** is seemingly always accompanied by the concomitant absorption of water, even for freshly dehydrated material. Thus, seeking to further explore the alcohol and water inclusion behavior, ***γ*-3** (or $\mathbf{3}\cdot 6H_2O$, the outcome was observed to be statistically the same) was immersed in various alcohols, allowed to equilibrate for 24 h, filtered, air-dried, dissolved in D_2O, and the extent of alcohol

Table 2. Alcohol/H_2O Absorption Properties of ***γ*-3**[a]

guest	equiv ROH absorbed[b]	% mass loss expected[c]	% mass loss observed[d]	equiv H_2O absorbed[e]
water				5.9
methanol	0.6	1.3	4.1	2.5
ethanol	1.4	4.1	6.0	1.5
1-propanol	2.0	7.4	10.4	3.0
2-propanol	2.5	9.0	11.3	2.4
1-butanol	2.2	9.7	10.8	1.2
2-butanol	1.9	8.4	10.7	2.5
t-butanol	0.4	1.7	8.3	6.0
1-pentanol	0.4	2.3	7.1	4.5
1-hexanol	0.0		nd[f]	nd[f]

[a]Equivalents are given per formula unit. [b]As determined by ^{1}H NMR. [c]Based upon equiv. ROH absorbed. [d]As determined by TGA. [e]Deduced from the difference between % mass loss observed and % mass loss expected, assuming the difference can be attributed to H_2O. [f]nd = not determined.

in the material determined by ^{1}H NMR spectroscopy. TGA was used to quantify the remaining water content by comparing the total observed mass loss to that expected based upon the alcohol stoichiometry that was accurately quantified by ^{1}H NMR. The results of these alcohol-water exchange studies are shown in Table 2.

Table 2 shows that only alcohols in the C2−C4 size range were appreciably absorbed (> 1 equiv) by ***γ*-3** and that water competes reasonably well with all alcohols. Though it was anticipated that, because of their size, larger alcohols would have difficulty in being reabsorbed, it was surprising to find that methanol was not significantly reabsorbed despite its intermediacy in size between water and ethanol. Straight chain butanol appears to be favored over its branched chain counterparts, 2-butanol and *tert*-butanol. Of the alcohols, ***γ*-3** has the greatest affinity for ethanol, 1-propanol (1-PrOH), 2-propanol (2-PrOH), 1-butanol (1-BuOH) and 2-butanol (2-BuOH). Among these, pairwise competition studies were conducted to more accurately determine the relative affinity of ***γ*-3** for these alcohols. ***γ*-3** was immersed in 1:1 molar solutions of competing alcohols for 24 h before being removed by filtration and examined by ^{1}H NMR. Interestingly, though the data in Table 2 seems to suggest that the inclusion of 2-PrOH might be favored relative to 1-PrOH, direct competition studies demonstrate that the straight chain alcohol is in fact preferentially included, with a modest selectivity of $K_{\text{1-PrOH: 2-PrOH}} = 1.7$.[48] Direct competition between 1-PrOH and ethanol also revealed 1-PrOH to be modestly preferred, with a selectivity coefficient of $K_{\text{1-PrOH:EtOH}} = 1.25$. Similar results were observed for the 1-PrOH/1-BuOH competition, with a selectivity coefficient measuring $K_{\text{1-PrOH:1-BuOH}} = 1.53$. Competition between 1-BuOH and 2-BuOH ($K_{\text{1-BuOH:2-BuOH}} = 2.5$) further illustrates the preference of ***γ*-3** for straight chain alcohols. In all, the low observed selectivity coefficients ($K_{\text{A:B}} < 2.5$) imply that ***γ*-3** only modestly discriminates between the various alcohols that can be included, though longer chain alcohols (> C5) are altogether excluded.

To ascertain whether the structural differences between ***γ*-3** and ***δ*-3** result in differences in selective alcohol inclusion behavior, similar alcohol/water sorption experiments were performed on ***δ*-3**. Somewhat surprisingly, the results for ***δ*-3** proved to be statistically similar to those obtained with ***γ*-3**, illustrating that the polymorphic apohosts ***γ*-3** and ***δ*-3** do not show appreciable differences in their guest-selective inclusion properties.

To determine what happens to the structure of ***γ*-3** and ***δ*-3** upon reabsorption of the alcohols, PXRD patterns of these materials were obtained after their immersion in ethanol. These PXRD patterns do not completely match those of **α-3-EtOH**, ***β*-3-DMF**, or the desolvated materials, ***γ*-3** or ***δ*-3**. Instead, the PXRD pattern of ethanol resolvated ***γ*-3** appears to be a hybrid of the patterns of ***γ*-3** and **α-3-EtOH**, exhibiting features from both the patterns. Similarly, the PXRD pattern of ethanol resolvated ***δ*-3** appears to be a hybrid of the patterns of ***δ*-3** and ***β*-3-DMF**. These observations may be attributed to the incomplete reabsorption of the ethanol within the frameworks and the presence of uncoordinated water molecules.

Conclusions

In conclusion, the $[CpFe]^+$ sandwich complex of terephthalic acid was isolated and fully characterized for the first time. It was easiest isolated as a 1:1 co-crystal between the $[PF_6]^-$ salt of its doubly protonated form, $H_2\mathbf{1}^+$, and its monoprotonated form, H**1**. The single crystal structures of H**1** and [H**1**·H_2**1**][PF_6] were determined. A series of 3D MOMF coordination polymers of the general formula $[M_3(\mathbf{1})_4(\mu\text{-}H_2O)_2(H_2O)_2][NO_3]_2\cdot x$solvent (M = Co^{II} (**2**), Ni^{II} (**3**); solvent = EtOH, or DMF/H_2O) were synthesized and fully characterized. These materials were shown by single crystal and PXRD to be polymorphic (and pesudopolymorphic), possessing identical 3D body-centered tetragonal network topologies, but differing in the manner by which the $[CpFe]^+$ groups are arranged within the 2D, square grid sheets of the networks. The polymorphism arises directly from the differentiation of the two arene faces of the terepthalate ligand by the $[CpFe]^+$ moieties, leading to the **α-2/3** frameworks, exhibiting an "in-in-out-out" arrangement of the $[CpFe]^+$ moieties, and the ***β*-2/3** frameworks, exhibiting an "in-out-in-out" arrangement. **α-2-EtOH**, ***β*-2-EtOH**, **α-3-EtOH**, ***β*-2-DMF**, and ***β*-3-DMF** were thermally desolvated, giving rise to isolable apohosts of composition $[M_3(\mathbf{1})_4(\mu\text{-}H_2O)_2(H_2O)_2][NO_3]_2$ (M = Co^{II} (**2**), Ni^{II} (**3**)) that were shown by PXRD to possess different, as yet unknown, crystal structures. The apohosts, namely, ***γ*-2** and ***δ*-2**, derived from **α-2-EtOH** and ***β*-2-EtOH**, respectively, were also found, however, to be polymorphic, apparently retaining at least some structural characteristics of the original polymorphic frameworks. The ability of the apohosts to be resolvated by alcohols and/or water was studied by exposing them to the appropriate vapors or immersing them in alcohols ranging in size from methanol to hexanol. ***γ*-3** showed a modest preference for the absorption of water and short chain, linear alcohols. The studies illustrated, for example, that apohosts ***γ*-3** and ***δ*-3** (obtained by the desolvation of **α-3-EtOH** and ***β*-3-DMF**, respectively)

(48) (a) Pivovar, A.; Holman, K.; Ward, M. *Chem. Mater.* **2001**, *13*, 3018; The selectivity of a material for the inclusion of compound A relative to compound B can be quantified by the selectivity coefficient, $K_{A:B}$, according to the equation $K_{A:B} = (K_{B:A})^{-1} = Y_A/Y_B \cdot X_B/X_A$ where X represents the initial mole fractions of the guests in solution phase and Y represents the mole fractions of the guests included by the material. In the experiments described herein, $X_A/X_B = 1$.

showed little appreciable difference in their selective inclusion of alcohols, each being modestly selective toward the uptake of 1-propanol.

Acknowledgment. This work was supported by the National Science Foundation (DMR-0349316) and the Department of Chemistry at Georgetown University. We thank Amy Cairns and Prof. Mohammed Eddaoudi of the University of South Florida for their gas sorption analyses of ***γ*-2**, ***δ*-2**, ***γ*-3**, and ***δ*-3**.

Supporting Information Available: General experimental details and characterization data. This material is available free of charge via the Internet at http://pubs.acs.org.